Accepted Manuscript

Synthesis of new heterocyclic compounds based on pyrazolopyridine scaffold and evaluation of their neuroprotective potential in MPP^+-induced neurodegeneration

Jabrane Jouha, Mohammed Loubidi, Jamila Bouali, Salha Hamri, Abderrafia Hafid, Franck Suzenet, Gérald Guillaumet, Taner Dagcı, Mostafa Khouili, Fadime Aydın, Luciano Saso, Güliz Armagan

PII: S0223-5234(17)30084-3

DOI: 10.1016/j.ejmech.2017.02.019

Reference: EJMECH 9215

To appear in: *European Journal of Medicinal Chemistry*

Received Date: 18 October 2016

Revised Date: 5 February 2017

Accepted Date: 7 February 2017

Please cite this article as: J. Jouha, M. Loubidi, J. Bouali, S. Hamri, A. Hafid, F. Suzenet, G. Guillaumet, T. Dagcı, M. Khouili, F. Aydın, L. Saso, G. Armagan, Synthesis of new heterocyclic compounds based on pyrazolopyridine scaffold and evaluation of their neuroprotective potential in MPP^+-induced neurodegeneration, *European Journal of Medicinal Chemistry* (2017), doi: 10.1016/j.ejmech.2017.02.019.

GRAPHICAL ABSTRACT

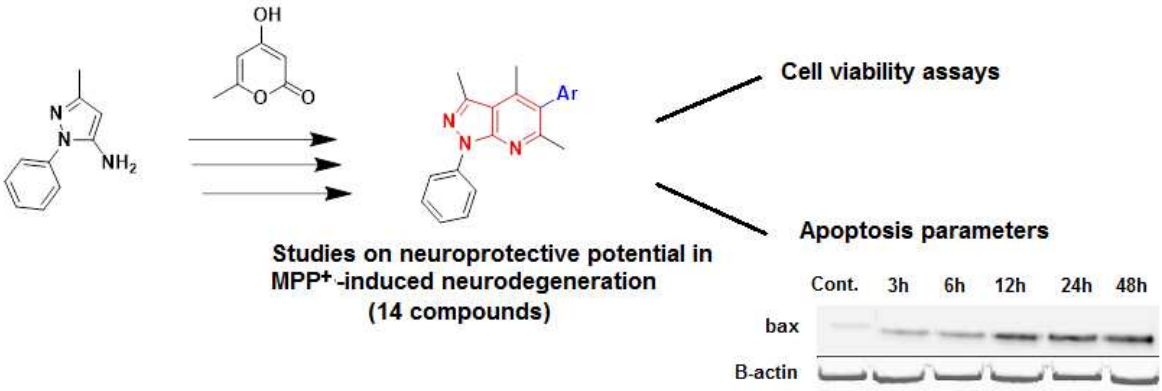

Synthesis of new heterocyclic compounds based on pyrazolopyridine scaffold and evaluation of their neuroprotective potential in MPP^+-induced neurodegeneration

Jabrane Jouha [a,b], Mohammed Loubidi [a], Jamila Bouali [b], Salha Hamri [b], Abderrafia Hafid [b], Franck Suzenet [a], Gérald Guillaumet [a], Taner Dagcı [c], Mostafa Khouili [b], Fadime Aydın [d], Luciano Saso [e], Güliz Armagan [d, *]

[a]Institut de Chimie Organique et Analytique, Université d'Orléans, UMR-CNRS 7311, BP 6759, rue de Chartres, 45067 Orléans cedex 2, France.

[b]Laboratoire de Chimie Organique et Analytique, Université Sultan Moulay Slimane - Faculté des Sciences et Techniques, BP 523, 23000 Beni-Mellal, Morocco.

[c]Department of Physiology and Center for Brain Research, Faculty of Medicine, Ege University, 35100 Bornova, Izmir, Turkey.

[d]Department of Biochemistry, Faculty of Pharmacy, Ege University, 35100 Bornova, Izmir, Turkey.

[e]Department of Physiology and Pharmacology "Vittorio Erspamer", Sapienza University of Rome, P. le Aldo Moro 5, 00185 Rome, Italy.

Corresponding author:

Güliz Armagan, Associate Professor

Department of Biochemistry, Faculty of Pharmacy, Ege University, 35100 Bornova, Izmir, Turkey.

guliz.armagan@ege.edu.tr Tel.: +90 532 383 06 93; Fax : +90 232 388 52 58

Abbreviations

MPP^+, 1-methyl-4-phenylpyridinium; SD, standard deviation; $NaHCO_3$, sodium bicarbonate; PE, petroleum ether; EtOAc, ethyl acetate; EtOH, ethanol; MeOH, methanol; BuOH, butanol; THF, tetrahydrofuran; NBS, N- bromosuccinimide

ABSTRACT:

Neurodegenerative disorders including Alzheimer's disease, Parkinson's disease, and Huntington's disease affect millions of people in the world. Thus several new approaches to treat brain disorders are under development. The aim of the present study is to synthesize potential neuroprotective heterocyclic compounds based on pyrazolopyridine derivatives and then to evaluate their effects in MPP^+-induced neurodegeneration in human neuroblastoma cell line (SH-SY5Y cells). The effects of the compounds on cell viability were measured by MTT assay and the changes in apoptosis-related proteins including bax, Bcl-2, Bcl-xl and caspase-3 were investigated by western blot technique. Based on the cell viability results obtained by MTT assay, the percentage of neuroprotection-induced by compounds against MPP^+-induced neurotoxicity in SH-SY5Y cells was between 20% and 30% at 5 µM concentrations of all synthesized compounds. Moreover, the downregulation in pro-apoptotic proteins including bax and caspase-3 were found following the novel synthesized compounds treatments and these effects were observed in a dose-dependent manner. Our results provide an evidence that these heterocyclic compounds based on pyrazolopyridine derivatives may have a role on dopaminergic neuroprotection via antiapoptotic pathways.

KEYWORDS: MPP^+, neurodegeneration, pyrazolo[3,4-*b*]pyridine, Suzuki-Miyaura, apoptosis.

1. Introduction

The interest for the synthesis of the pyrazolo[3,4-*b*]pyridines has increased in organic and pharmaceutical chemistry. This heterocyclic system is found in a number of molecules possessing biological and/or pharmacological properties. They show antibacterial, anti-malarial, anti-proliferative and anti-coagulant activities [1-7]. Many other remarkable applications are reported in the literature, such as the selective inhibition of Cyclin Dependent Kinase (CDK) by 1H-pyrazolo [3,4-*b*] pyridine "SQ-67563 and SQ-67454" (Fig. 1) [8-10]. These derivatives have also been used for the treatment of anxiety disorders associated with neuronal inhibition induced by γ-aminobutyric acid (GABA) such as LASSBio-872, LASSBio-873, LASSBio-981 a LASSBio-982, Tracazolate and Etazolate [11-15].

Parkinson's disease is the second most common neurodegenerative disorder affecting 6 million individuals worldwide. The molecular pathogenesis of neurodegenerative disorders is associated with mitochondrial dysfunction, oxidative stress, and apoptosis [16, 17]. Apoptosis is a genetically regulated process of cell deletion and plays an essential role in the maintenance of tissue homeostasis. The Bcl-2 family proteins constitute a critical point in the intrinsic pathway of apoptosis. MPTP (1-methyl-4-phenyl-1,2,3,6-tetrahydropyridine) and MPP^+ (1-methyl-4-phenylpyridinium) induced cellular death are the most common models for understanding Parkinson's disease. MPTP metabolizes to MPP^+ which is a toxic cation with a reaction that is catalyzed by monoamine oxidase B (MAO-B) in glial cells, MPP^+, interacts with "complex I" in the electron transport chain in the substantia nigra [18]. After it is taken into the cell by the dopamine transporter, it causes dopaminergic cell death. The production of free radicals following MPP^+ increases cell death, thereby inducing neuronal death and a syndrome resembling Parkinson's disease. As a result of the loss of dopaminergic neurons, the cortical control of movements is destroyed and Parkinson's symptoms occur in humans. Current therapies based on dopamine replacement such as chronic treatment with L-DOPA have severe side effects [19, 20, 21]. Thus several new approaches to treat Parkinson's disease are under development. However, molecular and cellular mechanisms underlying the pathogenesis of diseases should become clear before their use.

In this study, first we aim to synthesize potential neuroprotective heterocyclic compounds based on pyrazolopyridine derivatives and then to evaluate their neuroprotective and antiapoptotic effects in Parkinson's disease model. Human neuroblastoma cell line SH-SY5Y was employed and MPP^+ was used to generate PD model *in vitro*. Western blot analysis was

made to assess the apoptotic effect of MPP^+ on SH-SY5Y cells and the potential neuroprotective effects of the synthesized compounds.

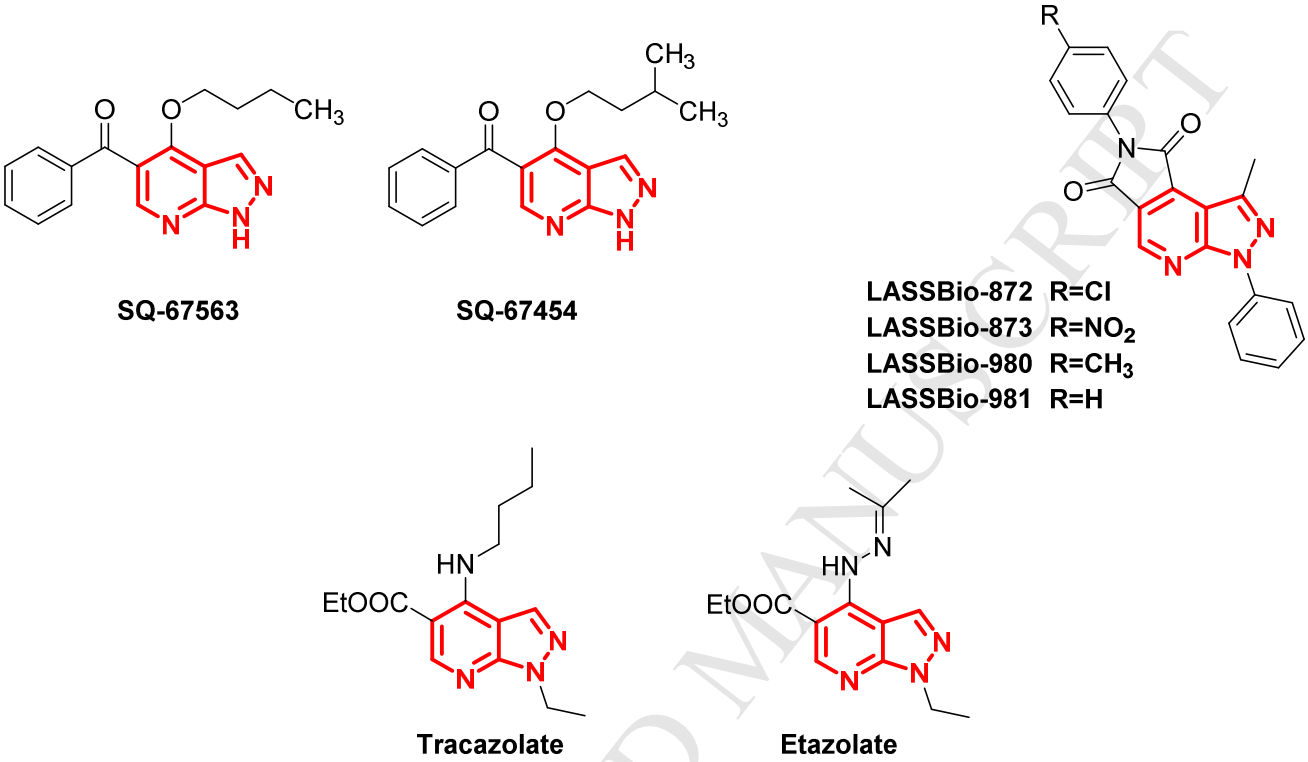

Fig. 1. Selected examples of pyrazolopyridine derivatives that can be used for potential therapies in the treatment of serious diseases.

2. Results and Discussion

2.1. Chemistry

Based on the interest of our research group in the synthesis of nitrogen-based heterocycles, we disclose herein the access to a library of original 3,4,6-trimethyl-1-phenyl-*1H*-pyrazolo[3,4-*b*]pyridine derivatives [22,23]. Our synthetic strategy is based on an efficient three-step synthesis of the bicycle followed by palladium catalyzed Suzuki–Miyaura cross-coupling. To the best of our knowledge, no example of palladium cross-coupling reaction on the 3,4,6-trimethyphenyl-*1H*-pyrazolo[3,4-*b*]pyridine substituted core has yet been reported. Our study was initiated by working on 3,4,6-trimethyl-1-phenyl-*1H*-pyrazolo[3,4-*b*]pyridine **3** (Scheme 1). This starting material was prepared from the commercially available 5-amino-1-phenyl-3-methylpyrazole **1** and 2-pyrone **2**.

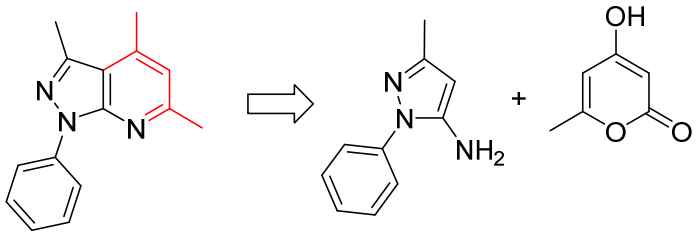

3 **1** **2**

Scheme 1

In this context, we first focused to optimize the condensation reaction between **1** and **2**. Initial reaction was conducted at 120 °C in sealed tube using 2 equiv of 2-pyrone **2** and methanol as solvent. Under these reaction conditions only 26% product **3** was isolated after 72h (Table 1, entry 1). Encouraged by this initial result, we decided to evaluate the influence of each reaction parameter such as catalyst, temperature and the type of solvent used. Results are summarized in Table 1. For example, *n*-butanol was found to be a convenient solvent (Table 1, entry 4). The presence of a catalyst, *p*-toluenesulfonic acid (PTSA) gave the product **3** with an excellent yield of 98% (Table 1, entry 5). On the contrary, MeOH, *n*-propanol and toluene lowered the yield and led predominantly to compound **3'** (Table 1, Entries 3, 6 and 7). Finally, replacing conventional thermal heating by microwave irradiation produced real improvement in terms of yield and time (Table 1, entry 2).

Table 1. Optimization of reaction condensation between **1** and **2**

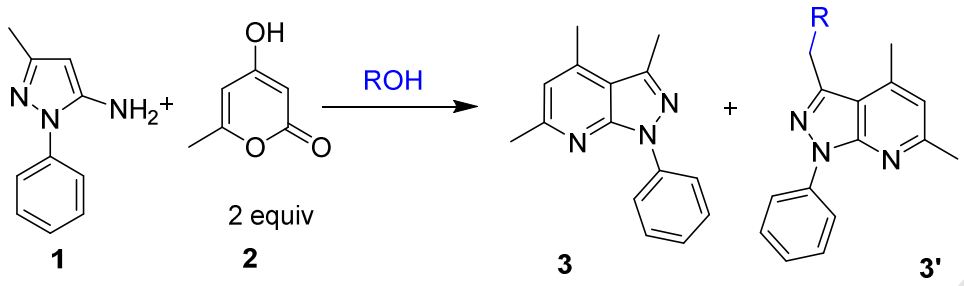

1 **2** **3** **3'**

Entry	Temperature [°C]	Solvent	Time [h]	Conversion [%][c]	Yield [%] [d]	Proportion of 3 and 3'	
						[%] of 3	[%] of 3'
1	120 [a]	CH_3OH	72h	37	26	0	100
2	140 [b]	CH_3OH	3h	100	64	33	67
3	140 [b]	CH_3OH / PTSA	3h	100	71	35	65
4	180 [b]	BuOH	3h	51	43	100	0
5	**180 [b]**	**BuOH / PTSA**	**3h**	**100**	**98**	**100**	**0**
6	140 [b]	*n*-C_3H_7OH/PTSA	3h	100	68	45	55
7	150 [b]	Toluene /PTSA	3h	100	40	100	0

[a] Sealed tube, [b] Microwave, [c] ^1H NMR ratio based on the integration of CH_3 (starting material), [d] Yield of isolated product after column chromatography

Regarding the synthesized intermediate **3**, one position remains potentially functionalizable (position 5), enlarging the potential molecular diversity offered by this synthon. First of all, bromination with N-bromosuccinimide afforded compound **4** with an excellent yield of 81% (Scheme 2).

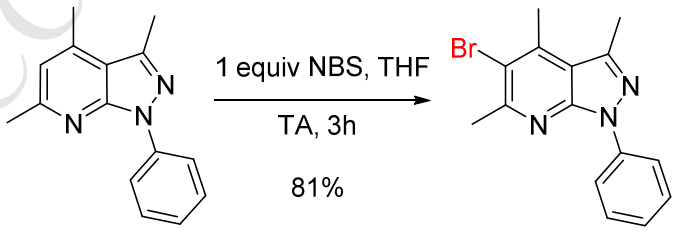

3 **4**

Scheme 2

Initial optimization trials of the Suzuki–Miyaura cross coupling reaction were performed on the pyrazolo[3,4-*b*]pyridine skeleton **4** synthesized previously using *p*-tolylboronic acid (Table 2). As a model, we began with the investigation using different palladium sources, (palladium(II) acetate or tetrakis(triphenylphosphine)palladium(0) as the catalyst, potassium carbonate as the base and a mixture of toluene/ethanol 2/1 as solvent. The coupling product **8** was obtained with acceptable yields (Table 2, entries 1 and 2). Without ethanol, even after 24h of heating, only 62% and 39% of conversion was achieved (Table 2, entries 6 and 7), showing that a protic solvent is essential in this coupling process. Replacing 1, 4-dioxane by toluene led to a significant decrease in conversion rate (Table 2, entries 3 and 4). The best conditions were found with a mixture of toluene/ethanol 2/1 as solvent. We next focused our attention on the influence of the catalyst. The use of palladium (0) instead a palladium(II) (i.e. $Pd(OAc)_2$, the yield significantly increased (Table 2, entry 1). To complete the optimization, we evaluated the impact of the amount of time and Pd $(PPh_3)_4$. The time of reaction could be reduced to 12 hours without impacting the yield of the reaction (Table 2, entry 5). On the other hand, the catalyst loading that could be reduced to 5 mol% of Pd $(PPh_3)_4$ did maintain a coupling efficiency (Table 2, entry 8).

To sum up, the best conditions were found to be tetrakis(triphenylphosphine)-palladium(0) (5 mol%), boronic acid (1.1equiv.), and sodium bicarbonate (1.5 equiv) in a mixture of toluene/ethanol 2/1, under reflux for 12 hours. To explore the scope of the methodology, we applied these selected conditions using different boronic acids. Gratifyingly, the optimized conditions proved to be efficient with boronic acids containing a large variety of functional groups. More precisely, *para*-substituted phenylboronic acids bearing electron-rich (CH_3, OCH_3, NM_2) or electron-poor (COOEt, NO_2, CF_3, CN, CHO, Cl) groups led to 5-aryl-1H- pyrazolo[3,4-*b*]pyridine in good yields (Table 3). Fortunately, the efficiency of our methodology was maintained using *ortho*- or *meta*-substituted aryl brororonic. The compounds **6** and **7** were isolated in good yields of 89% and 93%, respectively. Finally, heterocycles such as 3-thiophene and 2-fluoropyridine were introduced with good yields of 74% and 71% respectively (**17** and **18**).

Table 3. Scope of Suzuki–Miyaura cross coupling of **4**

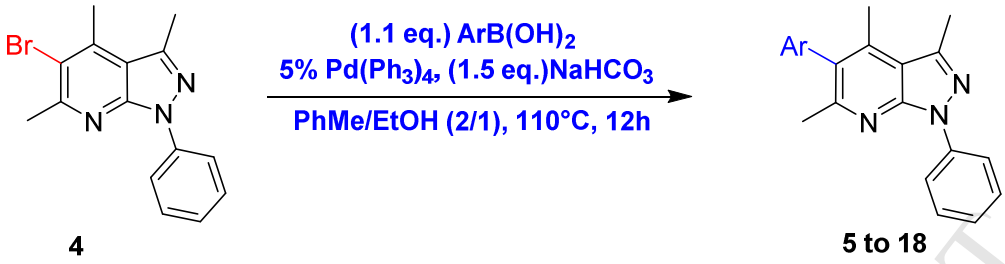

4 **5 to 18**

Entry	Product	Yield [%][a]	Entry	Product	Yield [%][a]
1	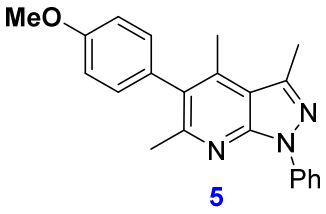 **5**	90	8	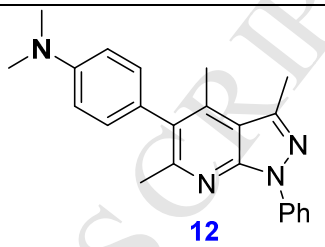 **12**	85
2	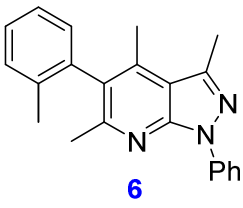 **6**	89	9	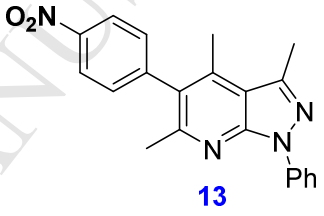 **13**	79
3	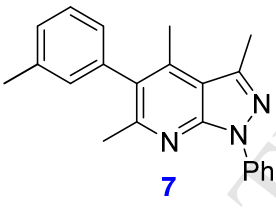 **7**	93	10	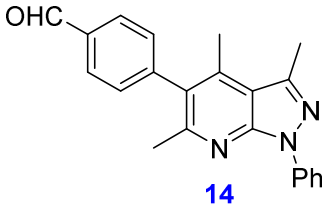 **14**	82
4	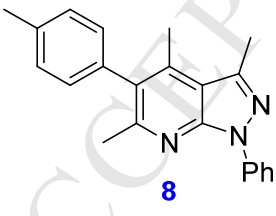 **8**	98	11	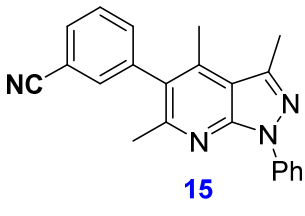 **15**	75
5	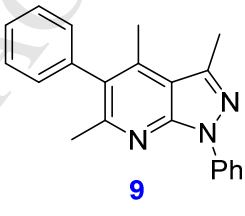 **9**	95	12	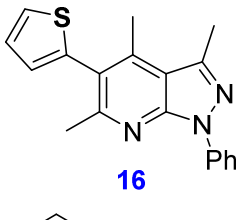 **16**	74
6	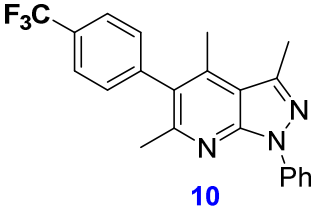 **10**	83	13	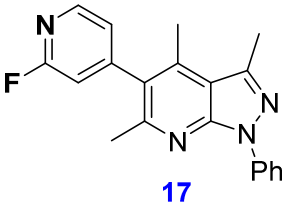 **17**	71

7	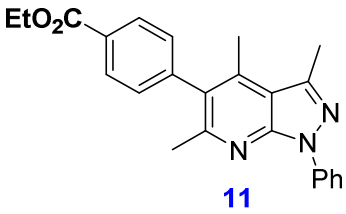 11	80	14	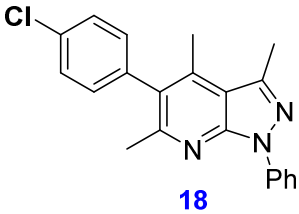 18	91

[a] Isolated yield after column chromatography

2.2. Biological studies

2.2.1. Cell viability studies

The cause of neurodegenerative diseases is still unknown and there is currently no standard treatment strategy for the patients. MPP^+ has been shown to selectively and potently inhibit complex I of the mitochondrial electron transport chain and to induce a PD-resembling syndrome in animals and cellular models [24, 25] therefore, it is often used as a classic neurotoxin to study PD development. In the current study, the neuroprotective effects of newly synthesized compounds were evaluated in a widely used cellular Parkinson's disease model in which neurotoxicity was induced by MPP^+ in cultured SH-SY5Y cells. It has been well established that SH-SY5Y cells are sensitive to the dopaminergic neuron toxin MPP^+. SH-SY5Y cells were treated with seven concentrations (0.1-10 mM) of MPP^+, and assayed for cytotoxicity after 12, 24, 36 and 48 h incubation by MTT assay. Fig. 2 shows that MPP^+ reduced the viability of SH-SY5Y cells in a time- and concentration-dependent manner. 0.2 mM MPP^+ induced a 11.8 ± 0.8%, a 21.5 ± 2.1% and a 27.1 ± 2.7% loss of cell viability at 24 h, 36 h and 48 h, respectively. 1 mM D-serine induced a 7.2 ± 0.5%, a 32.4 ± 3.4%, and a 46.3 ± 3.8% loss of cell viability at 12 h, 24 h and 36 h, respectively. 2 mM MPP+ significantly triggered the loss of cell viability at identical time ranges (12.2 ± 0.9% (12 h), 51.2 ± 3.1% (24 h), 67.1 ± 3.6% (36 h), 68.9 ± 1.7% (48 h), respectively). Both 10 mM and 5 mM concentrations of MPP^+ significantly induced cell death at 24, 36 and 48 hours. The percentage of cell viability was found nearly 10% following >5 mM MPP^+. In a study by Lee et al [26], the effect of MPP^+ on the viability of SH-SY5Y cells was assessed using alamarBlue assay. Similar to our findings, exposure of SH-SY5Y cells to MPP^+ resulted in a decrease in cell viability in a dose- and time-dependent manner. In our study model, since MPP^+ treatment for 24 h at 2 mM concentration was needed to yield dopaminergic damage, this exposure time was thus adopted in the following experiments.

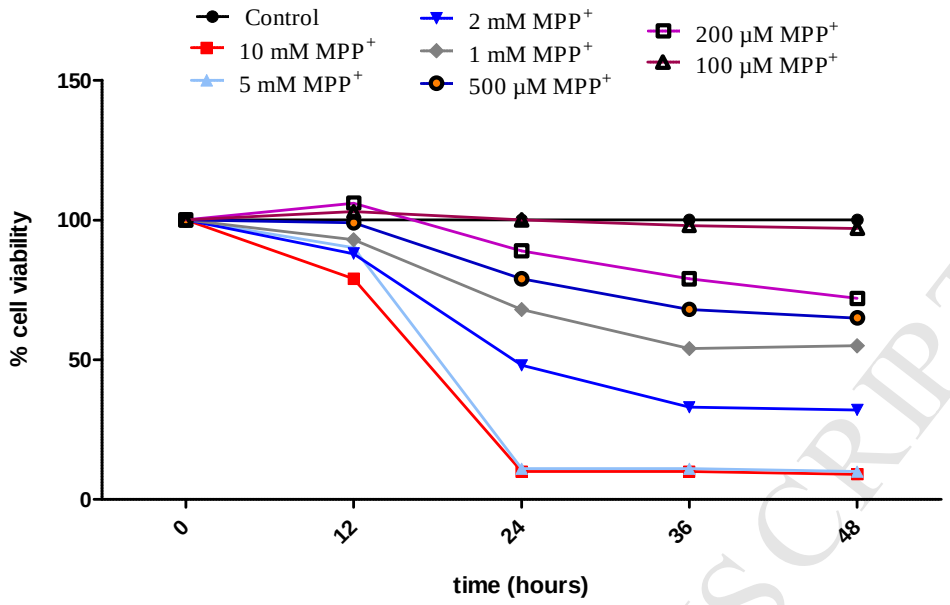

Fig. 2. Evaluation of cell viability of SH-SY5Y cells exposed to various concentrations (0.1-10 mM) of MPP^+ at indicated times. Cells were treated for 12, 24, 36 and 48 h at 37°C. Data represent the mean ± SD of at least six independent experiments in triplicate and are expressed as percentage of control cells.

To assess the effect of synthesized compounds on the proliferation of cells, we determined the cell activity of dehydrogenase enzymes by MTT assay at 3, 6 and 24 h after exposure. Cells cultured in compounds or control cells exhibited approximately the same proliferation rate, showing an increase in activity of dehydrogenase enzymes. Since MPP^+ treatment for 24 h at 2 mM concentration was needed to yield dopaminergic damage, this exposure time was thus adopted in the following experiments.

SH-SY5Y cells were pre-treated with compounds (5-20 µM) and then treated with MPP^+ (2 mM) to determine the dopaminergic cell death induced by MPP^+ and to evaluate the potential protective effects of newly synthesized compounds against MPP^+. We found that all concentrations of compounds (5-20 µM) considerably protect against MPP^+-induced neurotoxicity in a dose-dependent manner as evidenced by an increase in cell viability (Fig. 3). Moreover, most of the compounds at 5 µM provide higher than 25% neuroprotection (Table 4).

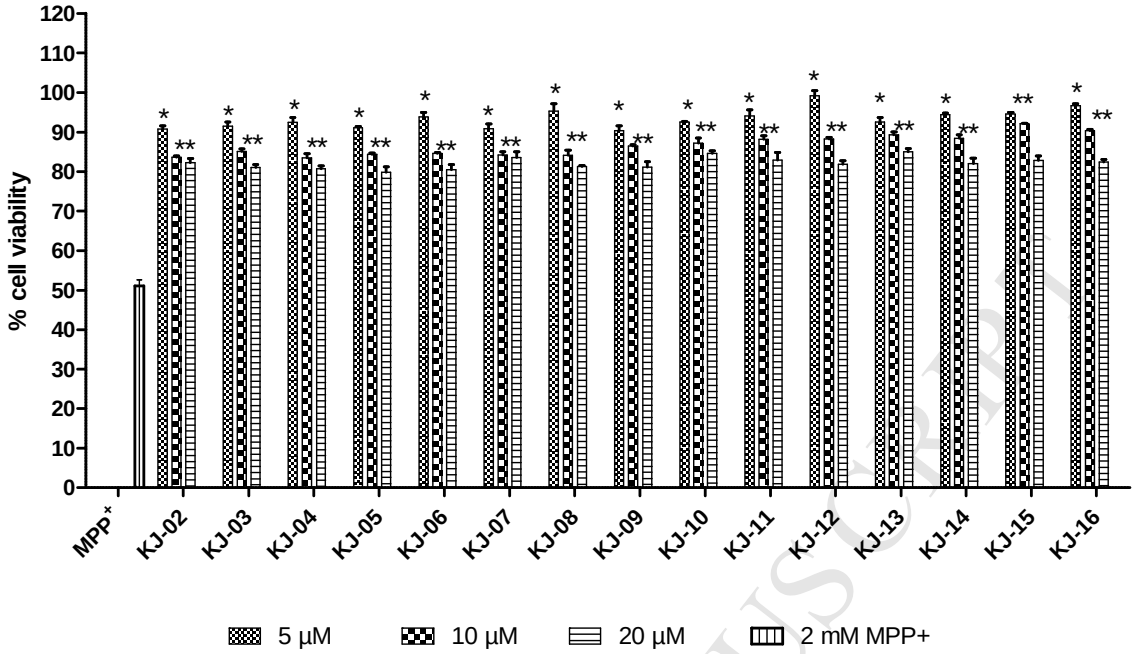

Fig. 3. Effects of newly synthesized compounds on cell viability in MPP^+-induced dopaminergic cell death. All values are means ± SDs (n = 5). * p<0.05 significant difference from MPP^+ and 10 or 20 µM concentrations of compound treatments. ** p<0.05 significant difference from MPP^+-treated cells.

Table 4. The percentage of neuroprotection-induced by compounds against MPP^+-induced neurotoxicity in SH-SY5Y cells.

Compound	% Neuroprotection	Compound	% Neuroprotection
4	* at 10 and 20 µM ** at 5 µM	**11**	* at 10 and 20 µM ** at 5 µM
5	* at 10 and 20 µM ** at 5 µM	**12**	* at 10 and 20 µM ** at 5 µM
6	* at 10 and 20 µM ** at 5 µM	**13**	* at 10 and 20 µM ** at 5 µM
7	* at 10 and 20 µM ** at 5 µM	**14**	* at 10 and 20 µM ** at 5 µM
8	* at 10 and 20 µM ** at 5 µM	**15**	* at 10 and 20 µM ** at 5 µM
9	* at 10 and 20 µM ** at 5 µM	**16**	* at 10 and 20 µM ** at 5 µM
10	* at 10 and 20 µM ** at 5 µM	**17**	** at 5 and 10 µM * at 20 µM
		18	** at 5 and 10 µM * at 20 µM

*Neuroprotection is between 10%-20%.

** Neuroprotection is between 20%-30%.

2.2.2. Protein analysis

According to the results obtained by cell viability analysis, the most effective compounds (**8**, **10**, **13**, **14**, **16** and **18**) were used for further analysis in order to understand their roles on apoptotic pathways in our study model. Apoptotic proteins including bax and caspase-3 and anti-apoptotic proteins including Bcl-2 and Bcl-xl were used as parameters of apoptosis. The time course of ultrastructural and biochemical changes surrounding cell death helps us to understand the mechanisms and potential therapeutic drugs can be found by defining these changes. In previous studies, it has been shown that the exposure of SH-SY5Y cells to MPP^+ resulted in an increase in apoptosis in a dose- and time-dependent manner [27]. In our study, in vitro apoptotic effects of MPP^+ were investigated at different time exposures (3-48h) (Fig. 4). Fall et al. [27] reported that SH-SY5Y cells undergo concentration-dependent apoptosis in response to MPP^+. At concentration sufficient to cause significant apoptosis within approximately one cell cycle (~19h) and apoptotic end stage became significant by 18 h. By

measuring the pro-apoptotic bax levels, we confirmed that MPP^+-induced apoptosis was observed before 18 hours and initiated at 12 hours.

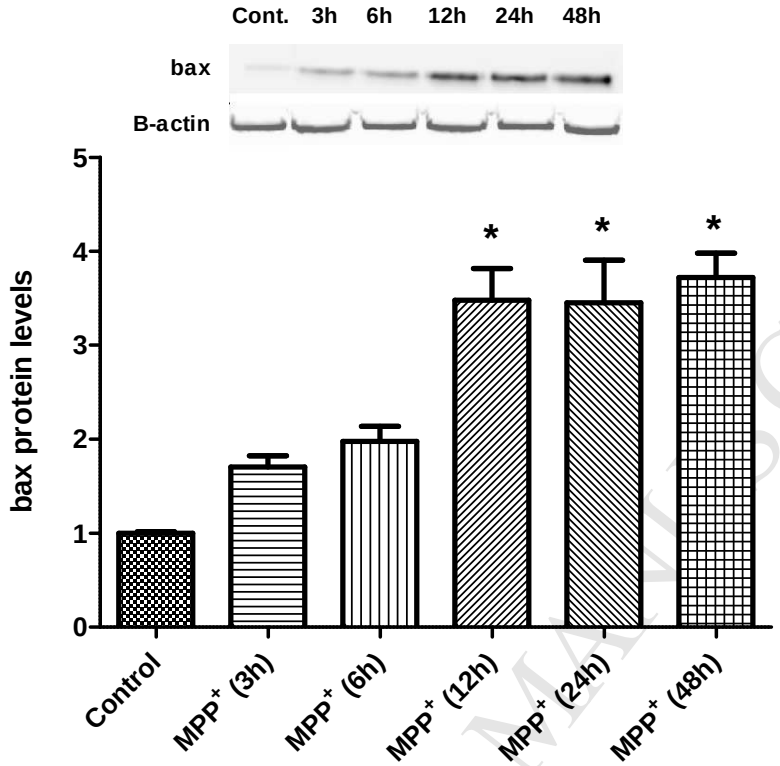

Fig. 4. The changes in proapoptotic bax protein levels following MPP^+ treatments for 3, 6, 12, 24, 48 h in SH-SY5Y cells. *$p \leq 0.05$ significant difference from control group and 3 or 6 hours MPP^+- treated cells.

The indicated exposure time (12h), as an initiation time for apoptosis for MPP^+, was adopted in the following experiments. Later, the newly synthesized compounds including **8**, **10**, **13**, **14**, **16** and **18** at the doses of 1 and 5 µM were investigated against MPP^+-induced apoptosis. In this study, we tried to find the lowest concentration of compounds that exerts protection. Thus, we have chosen the concentrations lower than used in MTT assay. It was suggested that the interplay between pro- and anti-apoptotic Bcl-2 family members may play a significant role in MPP^+-induced apoptotic cell death by regulating the permeability of the mitochondrial membrane and controlling the release of cytochrome c from mitochondria [28-30] Caspase-3 activation by released cytochrome c has been demonstrated to participate in MPP^+-induced apoptosis.

Similar to MTT assay, higher concentrations (5 µM) also significantly reversed the effects of MPP^+ on propoptotic and antiapoptotic proteins in our study model. Regarding to

proapoptotic protein bax, all groups decreased protein levels in consistent with concentrations following MPP^+ treatments when compared to MPP^+-treated cells (Fig. 5). Cells exposed to **8,10, 13, 14, 16**, and **18** had a decrease in bax levels from 1.26 fold to 0.49-, 0.86-, 1.03-, 0.82 and 0.68-fold at 5 µM, respectively. At 1 µM concentrations, fold changes in bax protein levels decreased to 1.11, 0.85, 0.75, 0.86, 0.76 and 0.78 ± 0.01. Among the compounds, **10** at 5 µM was found to be the most effective compound on bax protein levels. The expression of Bcl-2, an anti-apoptotic protein, was significantly decreased in MPP^+-treated cell (0.41 ± 0.02 fold variation to control) which supports the previous findings regarding to apoptotic effects of MPP^+ [31]. The anti-apoptotic protein Bcl-2 may be regulated in a dose-dependent manner by selected compounds. Because, an increase in Bcl-2 levels that is statistically significant was observed in the groups that were treated with compounds at the doses of 5 µM (2.84 ± 0.02, 3.62 ± 0.02, 0.85 ± 0.01, 3.22 ± 0.03, 2.63 ± 0.05, 4.33 ± 0.06, 0.39 ± 0.01 fold variation to control, respectively) (Fig. 5). However, the compounds at 1 µM did not have a significant effect on Bcl-2 protein levels (data not shown).

Caspase-3 is a critical inducer protein of apoptosis and the cleavage of the protein at Asp175 into the activated p17 and p19 fragments is required for the activation of it. After a 12-hour treatment of SH-SY5Y cells with 2 mM MPP^+, a significant increase in activated caspase-3 protein was detected compared to control cells (Fig. 5 and 6). When SH-SY5Y cells were exposed to 1 µM of compounds and 5 µM of **8** and **14** in the presence of 2 mM MPP^+, the cotreated cells showed a significant decrease in activated caspase-3 compared to the MPP^+ treatment alone (Fig. 5 and 6). On the other hand, it is found that the concentration is negatively correlated with caspase-3 and Bcl-xl protein levels for some compounds. For instance, lower concentrations of **10** and **13** (1 µM) on caspase-3 and Bcl-xl protein levels are more potent than higher concentrations. Similarly, **16** and **18** were found to decrease the levels of activated caspase-3 at low concentrations. Our results indicated that these compounds may induce and inhibit apoptosis in different manner. These findings support the usage of lower concentrations of **10** and **13** for the inhibition of caspase-3-mediated apoptosis and finally for neuroprotection.

Bcl-xl is an anti-apoptotic member of the Bcl-2 family and locates at the outer mitochondrial membrane and regulates outer mitochondrial membrane channel (VDAC) opening. To further confirm that the compounds are able to inhibit apoptosis in our study model, the levels of Bcl-xl are also measured following MPP^+ treatments. Bcl-xL protein levels were reduced with MPP^+ in SH-SY5Y cells 12 h after (0.27 ± 0.01 fold variation to control). When compared, lower doses of the compounds were found more effective in

increasing Bcl-xl levels. However, compound **10** at 5 µM failed to increase the levels of Bcl-xl in the presence of MPP^+ (Fig. 5) (0.27 ± 0.001 vs. 0.28 ± 0.01).

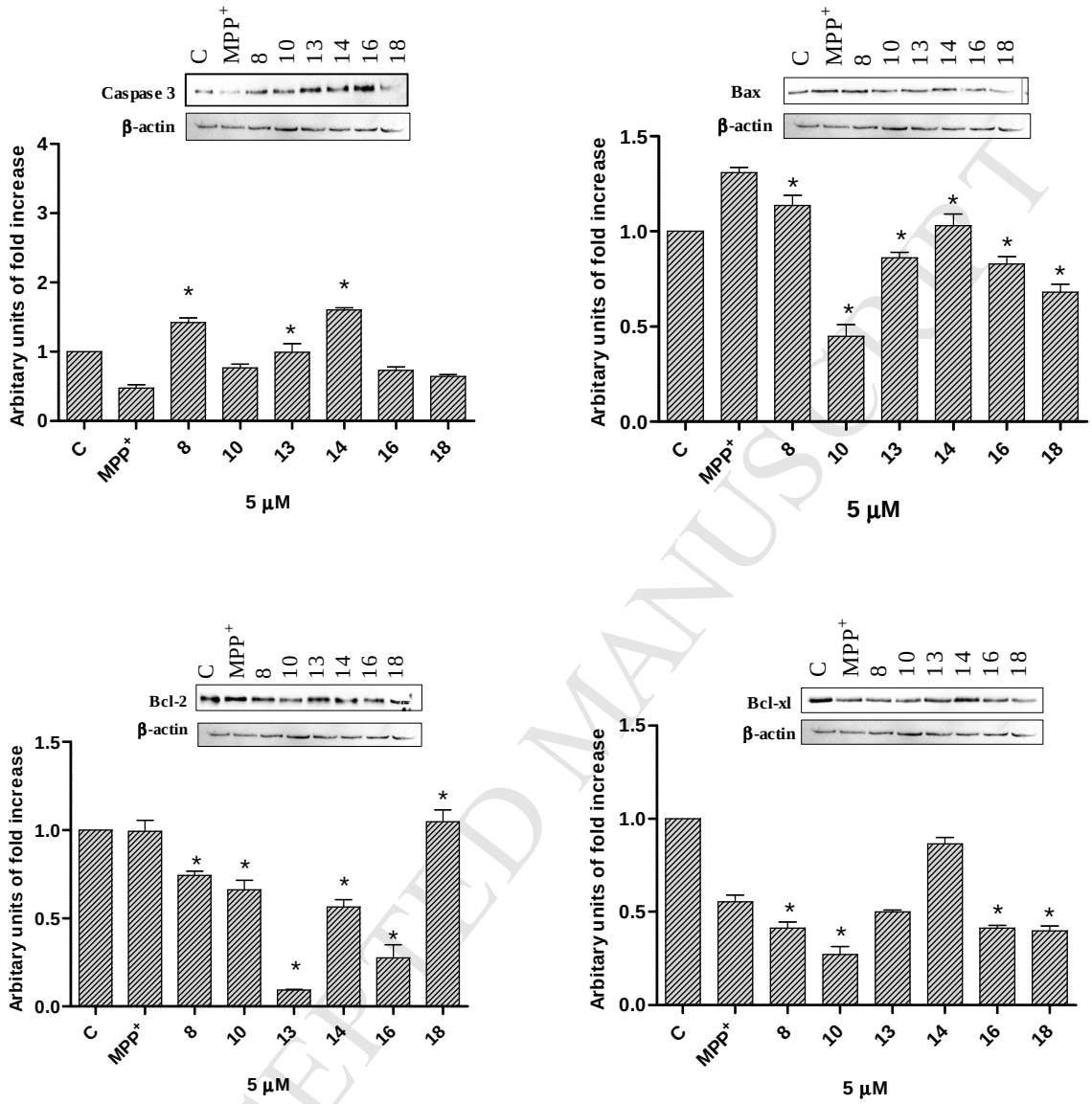

Fig. 5. The changes in bax, caspase-3, Bcl-2 and Bcl-xl protein levels following 5 µM **8**, **10**, **13**, **14, 16** or **18** against 2 mM MPP+-induced apoptosis. Representative Western blots showing protein expression of protein levels following treatments. Graphs indicate the relative densitometric values of indicated proteins. Quantification of protein product was performed by densitometric scanning. Data are normalized by using the β-actin signal and expressed as arbitrary densitometric units. Values are means ± SD; n = 3 in each group. *p<0.05 significant difference from MPP^+-treated cells.

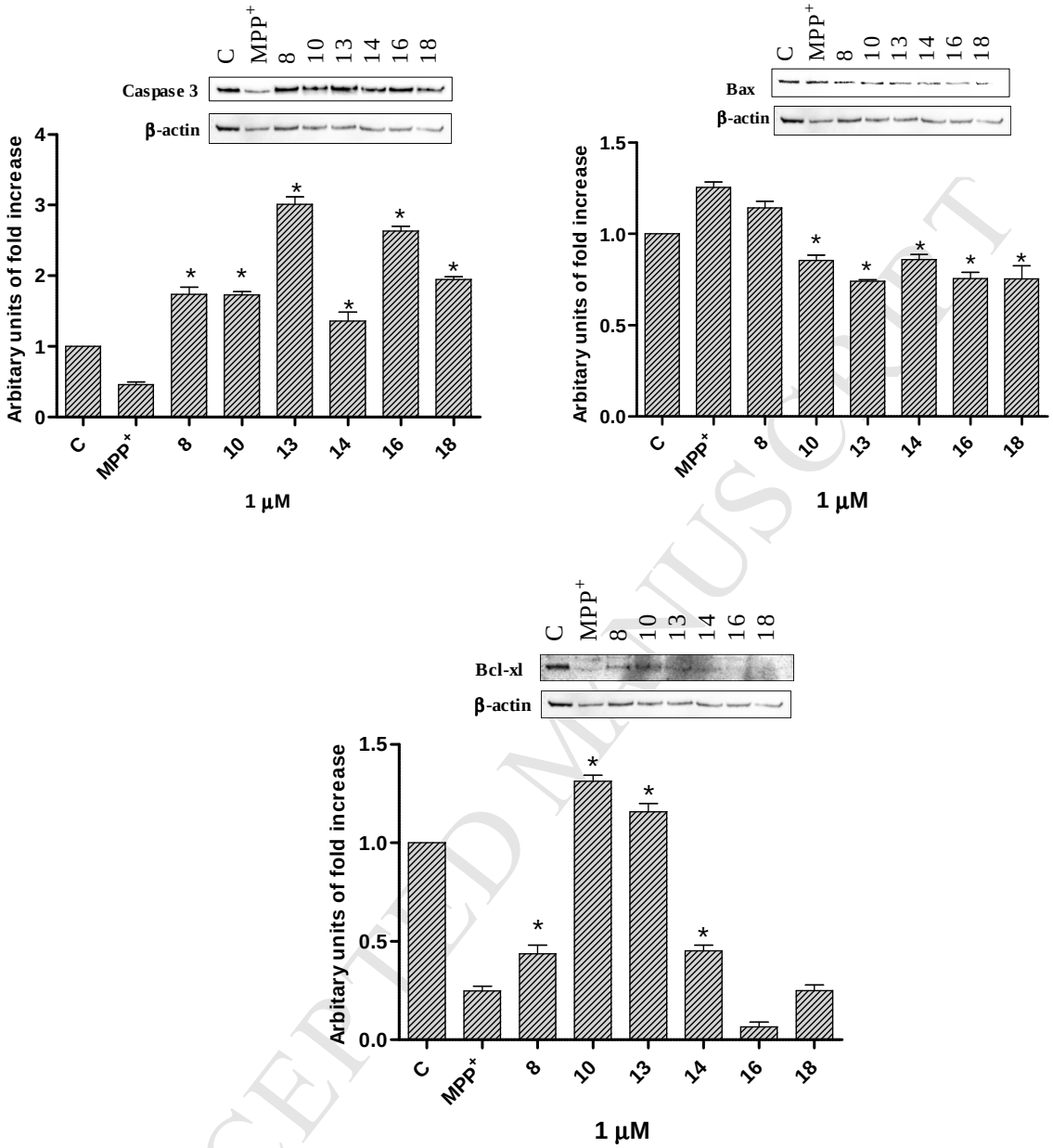

Fig. 6. The changes in bax, caspase-3 and Bcl-xl protein levels following 1 µM **8, 10, 13, 14, 16** or **18** against 2 mM MPP^+-induced apoptosis. Representative Western blots showing protein expression of protein levels following treatments. Graphs indicate the relative densitometric values of indicated proteins. Quantification of protein product was performed by densitometric scanning. Data are normalized by using the β-actin signal and expressed as arbitrary densitometric units. Values are means ± SD; n = 3 in each group. *p<0.05 significant difference from MPP^+-treated cells.

Today, several new approaches including diaesase-directed multitarget drugs, novel inhibitors to treat neurodegenerative disorders are under development [32-34]. We have here shown the neuroprotective effects of different chemical compounds in an *in vitro* model of dopaminergic cell death using the human neuroblastoma cell line SH-SY5Y. We show that all the compounds tested at indicated concentrations attenuated MPP^+-induced neuronal cell death as measured by cell viability assays. The percentage of neuroprotection-induced by compounds against MPP^+-induced neurotoxicity in SH-SY5Y cells was between 10%-20% at 20 and 50µM concentrations of compounds in **4** to **16** groups and at 20 µM concentrations of **17** and **18** groups. Moreover, 20%-30% neuroprotection was also observed at 5 µM concentrations of all compounds. These results are consistent with previous studies indicating that small heterocyclic compounds, an inhibitor of GSK-3, eliminated 6-OHDA-induced cellular death and apoptosis of SH-SY5Y cells [23]. Similarly, a pyrazole derivative of curcumin, CNB-001, increases cell viability following rotenone-induced toxicity [24]. Also, in our laboratory we have shown that inhibition of GSK-3β by tideglusib, a thiadiazolidinone compound, prevent cell death induced by D-serine/NMDA in the developing brain and result in neuroprotection [25]. Moreover, we have confirmed the neuroprotection by **8**, **10**, **13**, **14**, **16** and **18** in *in vitro* Parkinson's disease model by measuring pro- and anti-apoptotic protein levels. The significant changes in these proteins support the idea that these selected compounds may have important roles in cell death mechanisms. Taken together, our results suggest that during *in vitro* MPP^+ toxicity, apoptotic pathways are among the targets for the neuroprotective action exerted by pyrazolopyridine derivatives.

3. Conclusion

In conclusion, our results provide an evidence that these heterocyclic compounds based on pyrazolopyridine scaffold have a role on dopaminergic neuroprotection. The neuroprotection of the compounds against MPP^+-induced apoptosis may be associated with the regulation of pro- and anti-apoptotic proteins, oxidative stress and downregulation of caspase-3 activation. According to our results, we suggest that these compounds, particularly most active ones, can be used for potential novel therapies in the treatment of Parkinson's disease.

4. Experimental Protocols

4.1. General Synthetic Methods

All reagents were purchased from commercial suppliers and were used without further purification. The purity (≥ 95 %) of final compounds was verified by ^{1}H and ^{13}C NMR analysis, melting point and HRMS. The reactions were monitored by thin-layer chromatography (TLC) analysis by using silica gel (60 F254) plates. Compounds were visualized by UV irradiation at 256 or 365 nm. Flash column chromatography was performed on silica gel 60 (230–400 mesh, 0.040–0.063 mm). Melting points (m.p. [°C]) were taken on samples in open capillary tubes and are not corrected. Infrared spectra of compounds were recorded with a Thermo Scientific Nicolet iS10 instrument. ^{1}H and ^{13}C NMR spectra were recorded with a Bruker spectrometer at 250 MHz (^{13}C, 61.5 MHz) or 400 MHz (^{13}C, 101 MHz). Chemical shifts are given in parts per million (ppm) from tetramethylsilane (TMS) as internal standard in $CDCl_3$, and the residual peak of DMSO in [D_6] DMSO. The following abbreviations are used for the ^{1}H NMR spectra multiplicities: br. s: broad singlet, s: singlet, d: doublet, t: triplet, q: quartet, qt: quintuplet, m: multiplet. Coupling constants (*J*) are reported in Hertz [Hz]. C_{IV} is the abbreviation for quaternary carbon atoms. High-resolution mass spectra (HRMS) were performed with a Maxis Bruker 4G instrument.

*4.1.1. 3,4,6-Trimethyl-1-phenyl-1H-pyrazolo[3,4-b]pyridine (**3**)*

To a solution of 4-hydroxy-6-methylpyran-2-one **2** (291 mg, 2.309 mmol) and 5-amino-3-methyl-1-phenylpyrazole **1** (200 mg, 1.154 mmol) in 10 ml of *n*-butanol was added *p*-toluenesulfonic acid (0.12 mg).The reaction mixture was submitted to microwave irradiation with stirring at 180 °C for 3 hour. It was then cooled to room temperature, and n-butanol was removed under reduced pressure. The crude product was purified by flash chromatography on silica gel (95:5 petroleum ether / ethyl acetate) to afford compound **3** as a white crystals. (390 mg; 98%); mp: 129-131 °C, IR (neat): ῡ= 3034.81, 2919.16, 1398.44, 1625.15, 1138.83, 776.94, 769.32 cm^{-1}. ^{1}H NMR (400 MHz, $CDCl_3$-*d*) δ 8.27 (d, *J* = 9 Hz, 2H), 7.48 (dd, *J* = 9.0, 6.0 Hz, 2H), 7.24 (d, 6.0 Hz, 1H), 6.80 (s, 1H,), 2.72 (s, 3H), 2.66 (s, 3H), 2.64 (s, 3H); ^{13}C NMR (101 MHz, $CDCl_3$-*d*) δ 158.8, 151.3, 142.6, 142.4, 139.8, 128.9, 125.2, 120.9, 118.6 , 114.6, 24.8, 18.9, 15.3; HRMS (ESI) calcd *m/z* for $[M + H]^+$ $C_{15}H_{16}N_3$ 238.1266, found 238.1263.

*4.1.2. 5-Bromo-3,4,6-trimethyl-1-phenyl-1H-pyrazolo[3,4-b]pyridine (**4**)*

To a solution of 3,4,6-trimethyl-1-phenyl-1*H*-pyrazolo[3,4-b]pyridine **3** (500 mg, 2.11 mmol) in 13 mL of THF was added, N-bromosuccinimide (375.01 mg, 2.11 mmol, 1.0 equiv.) The reaction mixture was stirred at room temperature for 3h before being quenched with an aqueous saturated solution of sodium thiosulfate (15 mL) and extracted with dichloromethane (3X10 mL). The combined organic layers were washed with water, dried over magnesium sulfate, filtered off and concentrated under reduced pressure. The residue was purified by flash chromatography (petroleum ether/ethyl acetate 8/2) to afford compound **4** as a white solid. (540 mg; 81%); mp: 169-171 °C, IR (neat): ῡ= 3028.78, 2940.18, 1643.26, 1478.76, 1239.54, 1077.31cm^{-1} . ^{1}H NMR (400 MHz, $CDCl_3$-*d*) δ 8.25 (d, *J* = 8.2 Hz, 2H), 7.48 (dd, *J* = 8.2, 7.4 Hz, 2H), 7.29 (d, 1H, 7.4 Hz, 1H), 2.80 (s, 3H), 2.76 (s, 3H), 2.73 (s, 3H); ^{13}C NMR (101 MHz, $CDCl_3$-*d*) δ 157.2, 149.0, 142.1, 141.9, 139.4, 128.9, 125.5, 120.8, 117.3 , 116.0, 27.2, 19.6, 15.7; HRMS (ESI) calcd *m/z* for $[M + H]^+$ $C_{15}H_{15}BrN_3$ 318.0610, found 318.0607.

<u>*General procedure:*</u> Suzuki Coupling on pyrazolo[3,4-*b*]pyridine **4** A flask containing a stirring bar was charged with the 5-bromo-3,4,6-trimethyl-1-phenyl-1*H*-pyrazolo[3,4-b]pyridine **4** (100 mg ; 0.31 mmol), boronic acid (1.1 equiv. 0.35 mmol) and sodium bicarbonate (1.5 equiv. 0.47 mmol) in a mixture of toluene/ ethanol (2/1 v/v). $Pd(PPh_3)_4$ (0.05 equiv. 0.018 mmol) was added and the mixture was refluxed for indicated time. After cooling down, solvents were removed under reduced pressure and the residue was purified by flash chromatography to provide the desired products **5** to **18**.

4.1.3. 5-(4-Methoxyphenyl)-3,4,6-trimethyl-1-phenyl-1*H*-pyrazolo[3,4-*b*]pyridine *(**5**)*

Following the general procedure with 4-methoxyphenylboronic acid (52 mg, 0.35 mmol) the mixture was refluxed for 12 hours. The crude product was purified by flash chromatography on silica gel (90:10 petroleum ether / ethyl acetate) to afford compound **5** as a white solid. (98 mg; 90%); mp: 144-146 °C, IR (neat): ῡ= 3024.93, 1633.61, 1382.94, 1205.15, 771.84, 752.73 cm^{-1}, ^{1}H NMR (400 MHz, $CDCl_3$-*d*) δ 8.33 (d, *J* = 8.1 Hz, 2H), 7.55 – 7.42 (m, 2H), 7.25 (d, *J* = 6.4 Hz, 1H), 7.09 (d, *J* = 7.7 Hz, 2H), 7.00 (d, *J* = 8.1 Hz, 2H), 3.88 (s, 3H), 2.75 (s, 3H), 2.39 (s, 3H), 2.38 (s, 3H); ^{13}C NMR (101 MHz, $CDCl_3$-*d*) δ 158.8, 157.9, 149.9, 142.7, 140.6, 139.8, 131.2, 130.9, 130.8, 128.9, 125.1, 120.7, 114.8, 114.1, 55.3, 25.3, 16.7, 15.8; HRMS (ESI) calcd *m/z* for $[M + H]^+$ $C_{22}H_{22}N_3O$ 344.1685, found 344.1684.

*4.1.4. 3,4,6-Trimethyl-1-phenyl-5-(o-tolyl)-1H-pyrazolo[3,4-b]pyridine (**6**)*

Following the general procedure with 2-tolylboronic acid (47 mg, 0.35 mmol) the mixture was refluxed for 12 hours. The crude product was purified by flash chromatography on silica gel (90:10 petroleum ether / ethyl acetate) to afford compound **6** as a white solid.

(92 mg; 89%); mp: 122-124 °C, IR (neat): ῡ= 3051.87, 2923.06, 1510.95, 1238.42, 757.10, 747.34, 672.88, 577.64 cm^{-1}. ^{1}H NMR (250 MHz, $CDCl_3$-*d*) δ 8.32 (dd, *J* = 8.7, 1.1 Hz, 2H), 7.53 – 7.43 (m, 2H), 7.34 – 7.26 (m, 3H), 7.25 – 7.19 (m, 1H), 7.10 – 6.96 (m, 1H), 2.74 (s, 3H), 2.30 (s, 3H), 2.28 (s, 3H), 1.98 (s, 3H); ^{13}C NMR (63 MHz, $CDCl_3$-*d*) δ 157.4, 150.2, 142.7, 140.3, 139.8, 138.4, 136.5, 130.3, 130.2, 129.8, 128.9, 127.7, 126.4, 125.1, 24.7, 19.6, 16.3, 15.7; HRMS (ESI) calcd *m/z* for $[M + H]^+$ $C_{22}H_{22}N_3$ 328.1735, found 328.1733.

*4.1.5. 3,4,6-Trimethyl-1-phenyl-5-(m-tolyl)-1H-pyrazolo[3,4-b]pyridine (**7**)*

Following the general procedure with 3-tolylboronic acid (47 mg, 0.35 mmol) the mixture was refluxed for 12 hours. The crude product was purified by flash chromatography on silica gel (90:10 petroleum ether / ethyl acetate) to afford compound **7** as a white solid. (96 mg; 93%); mp: 125-127 °C, IR (neat): ῡ= 2924.88, 1493.11, 1332.54, 1255.65, 791.90, 742.23, 699.50 cm^{-1}. ^{1}H NMR (250 MHz, $CDCl_3$-*d*) δ 8.33 (dd, *J* = 8.7, 1.1 Hz, 2H), 7.49 (t, *J* = 8.0 Hz, 2H), 7.36 (t, *J* = 7.4 Hz, 1H), 7.31 – 7.16 (m, 2H), 6.98 (d, *J* = 7.8 Hz, 2H), 2.42 (s, 3H), 2.39 (s, 3H), 2.37 (s, 3H), 2.35 (s, 3H); ^{13}C NMR (63 MHz, $CDCl_3$-*d*) δ 157.5, 150.0, 142.7, 140.2, 139.8, 139.0, 138.3, 131.3, 128.9, 128.6, 128.0, 127.9, 126.8, 125.1, 120.8, 114.7, 25.3, 21.5, 16.8 , 15.8; HRMS (ESI) calcd *m/z* for $[M + H]^+$ $C_{22}H_{22}N_3$ 328.1735, found 328.1730.

*4.1.6. 3,4,6-Trimethyl-1-phenyl-5-(p-tolyl)-1H-pyrazolo[3,4-b]pyridine (**8**)*

Following the general procedure with 4-tolylboronic acid (47 mg, 0.35 mmol) the mixture was refluxed for 12 hours. The crude product was purified by flash chromatography on silica gel (90:10 petroleum ether / ethyl acetate) to afford compound **8** as a white solid. (101 mg; 98%); mp: 131-133 °C, IR (neat): ῡ= 2920.63, 1493.27, 1335.78, 1253.14, 791.51, 739.98, 699.76 cm^{-1}.^{1}H NMR (400 MHz, $CDCl_3$-*d*) δ 8.33 (d, *J* = 8.0 Hz, 2H), 7.48 (t, *J* = 7.2 Hz, 2H), 7.32 – 7.18 (m, 4H), 7.06 (d, *J* = 7.2 Hz, 2H), 2.74 (s, 3H), 2.43 (s, 3H), 2.37 (s, 6H) ; ^{13}C NMR (101 MHz, $CDCl_3$-*d*) δ 157.6, 150.0, 142.7, 140.4, 139.9, 136.9, 136.0, 131.2, 129.7, 129.4, 128.9, 125.1, 120.8, 114.8, 25.3, 21.3, 16.7, 15.7; HRMS (ESI) calcd *m/z* for $[M + H]^+$ $C_{22}H_{221}N_3$ 328.1735, found 328.1731.

*4.1.7. 3,4,6-Trimethyl-1,5-diphenyl-1H-pyrazolo[3,4-b]pyridine (**9**)*

Following the general procedure with phenylboronic acid (42 mg, 0.35 mmol) the mixture was refluxed for 12 hours. The crude product was purified by flash chromatography on silica gel (90:10 petroleum ether / ethyl acetate) to afford compound **9** as a yellow solid. (94 mg; 95%); mp: 134-136 °C, IR (neat): ν̃= 3050.43, 3030.67, 2919.91, 1602.59, 987.35, 690.12 cm^{-1}, ^{1}H NMR (400 MHz, $CDCl_3$-*d*) δ 8.34 (d, *J* = 8.0 Hz, 2H), 7.56 – 7.44 (m, 4H), 7.42 (d, *J* = 6.8 Hz, 1H), 7.26 (t, *J* = 7.4 Hz, 1H), 7.20 (d, *J* = 7.4 Hz, 2H), 2.76 (s, 3H), 2.39 (s, 6H) ; ^{13}C NMR (101 MHz, $CDCl_3$-*d*) δ 157.5, 150.1, 142.9, 140.5, 139.9, 139.2, 131.4, 130.1,

129.1, 128.9, 127.4, 125.3, 121.0, 114.9, 25.4, 16.9, 15.9; HRMS (ESI) calcd *m/z* for [M + H]$^+$ $C_{21}H_{20}N_3$ 314.1579, found 314.1584.

*4.1.8. 3,4,6-Trimethyl-1-phenyl-5-(4-(trifluoromethyl)phenyl)-1H-pyrazolo[3,4-b]pyridine (**10**)*

Following the general procedure with 4-(trifluoromethyl)phenylboronic acid (66 mg, 0.35 mmol) the mixture was refluxed for 12 hours. The crude product was purified by flash chromatography on silica gel (90:10 petroleum ether / ethyl acetate) to afford compound **10** as a white solid. (100 mg; 83%); mp: 176-178 °C, IR (neat): ῡ= 3036.18, 2916.28, 1368.79, 1322.90, 1105.76, 1067.27, 846.16, 771.94, 739.55 cm^{-1}. ^{1}H NMR (250 MHz, $CDCl_3$-*d*) δ 8.32 (dd, *J* = 8.7, 1.1 Hz, 2H), 7.74 (d, *J* = 8.0 Hz, 2H), 7.58 – 7.42 (m, 2H), 7.33 (d, *J* = 7.9 Hz, 2H), 7.25 (s, 1H), 2.76 (s, 3H), 2.37 (s, 3H), 2.35 (s, 3H); ^{13}C NMR (63 MHz, $CDCl_3$-*d*) δ 156.9, 150.3, 143.3, 142.9, 140.4, 139.8, 130.5, 129.9, 129.9 (q, $^2J_{C\text{-}C\text{-}F}$ = 32.3 Hz),129.1, 125.9 (q, $^3J_{CHAr\text{-}F}$ = 3.7 Hz, C_{HAr}), 125.5, 123.7 (q, $^1J_{C\text{-}F}$ = 272.2 Hz, CF_3), 121.0, 114.8, 25.4, 16.9, 15.9; HRMS (ESI) calcd *m/z* for [M + H]$^+$ $C_{22}H_{19}F_3N_3$ 382.1453, found 382.1455.

*4.1.9. Ethyl-4-(3,4,6-trimethyl-1-phenyl-1H-pyrazolo[3,4-b]pyridin-5-yl)benzoate (**11**)*

Following the general procedure with 4-ethoxycarbonylphenylboronic acid (67 mg, 0.35 mmol) the mixture was refluxed for 12 hours. The crude product was purified by flash chromatography on silica gel (90:10 petroleum ether / ethyl acetate) to afford compound **11** as a brown solid. (98 mg; 80%); mp: 149-151 °C, IR (neat): ῡ= 3010.11, 2831.52, 1590.39, 1317.87 cm^{-1}. ^{1}H NMR (400 MHz, $CDCl_3$-*d*) δ 8.32 (d, *J* = 8.2 Hz, 2H), 8.19 (d, *J* = 7.8 Hz, 2H), 7.50 (t, *J* = 7.8 Hz, 2H), 7.36 – 7.06 (m, 3H), 4.43 (q, *J* = 7.1 Hz, 2H), 2.75 (s, 3H), 2.39 (s, 3H), 2.36 (s, 3H), 1.44 (t, *J* = 7.1 Hz, 3H) ; ^{13}C NMR (101 MHz, $CDCl_3$-*d*) δ 166.6, 156.9, 150.2, 144.3, 142.9, 140.3, 139.8, 130.4, 130.2, 130.1, 129.8, 129.1, 125.4, 121.0, 114.8, 61.3, 25.4 , 16.9, 15.9, 14.5; HRMS (ESI) calcd *m/z* for [M + H]$^+$ $C_{24}H_{24}N_3O_2$ 386.1790, found 386.1788.

*4.1.10. N,N-Dimethyl-4-(3,4,6-trimethyl-1-phenyl-1H-pyrazolo[3,4-b]pyridin-5-yl)aniline (**12**)*

Following the general procedure with 4-(dimethylamino)phenylboronic acid (57 mg, 0.35 mmol) the mixture was refluxed for 12 hours. The crude product was purified by flash chromatography on silica gel (90:10 petroleum ether / ethyl acetate) to afford compound **12** as a white solid. (96 mg; 85%); mp: 146-148 °C, IR (neat): ῡ= 3047.90, 2926.21, 1312.51, 1115.82, 1087.19 cm^{-1}. ^{1}H NMR (250 MHz, $CDCl_3$-*d*) δ 8.33 (d, *J* = 7.7 Hz, 2H), 7.49 (t, *J* = 8.0 Hz, 2H), 7.25 (d, *J* = 5.1 Hz, 1H), 7.03 (d, *J* = 8.8 Hz, 2H), 6.82 (d, *J* = 8.8 Hz, 2H), 3.02 (s, 6H), 2.75 (s, 3H), 2.42 (s, 3H), 2.40 (s, 3H) ; ^{13}C NMR (63 MHz, $CDCl_3$-*d*) δ 158.5, 150.0,

149.7, 142.9, 140.9, 140.0, 131.5, 130.6, 129.1, 126.8, 125.2, 120.9, 115.0, 112.7, 40.7, 25.6, 16.9, 15.9; HRMS (ESI) calcd *m/z* for $[M + H]^+$ $C_{23}H_{25}N_4$ 357.2001, found 357.2007.

*4.1.11. 3,4,6-Trimethyl-5-(4-nitrophenyl)-1-phenyl-1H-pyrazolo[3,4-b]pyridine (**13**)*

Following the general procedure with *p*-nitrophenylboronic acid (58 mg, 0.35 mmol) the mixture was refluxed for 12 hours. The crude product was purified by flash chromatography on silica gel (90:10 petroleum ether / ethyl acetate) to afford compound **13** as a yellow solid. (89 mg; 79%); mp: 157-159 °C, IR (neat): ῡ= 3027.66, 2850.12, 1519.07, 1337.16, 1036.77, 1020.35, 815.37, 698.90 cm^{-1} .^{1}H NMR (250 MHz, $CDCl_3$-*d*) δ 8.36 (d, *J* = 8.8 Hz, 2H), 8.31 (dd, *J* = 8.8, 1.1 Hz, 2H), 7.57 – 7.45 (m, 2H), 7.41 (d, *J* = 8.8 Hz ,2H), 7.34 – 7.20 (m, 1H), 2.76 (s, 3H), 2.38 (s, 3H), 2.35 (s, 3H). ^{13}C NMR (63 MHz, $CDCl_3$-*d*) δ 156.4, 150.3, 147.5, 146.7, 142.9, 140.3,140.1, 139.7, 131.2, 129.1, 125.6, 124.2, 121.0, 114.8, 25.4, 16.91 , 15.9; HRMS (ESI) calcd *m/z* for $[M + H]^+$ $C_{21}H_{19}N_4O_2$ 359.1430, found 359.1432.

*4.1.12. 4-(3,4,6-Trimethyl-1-phenyl-1H-pyrazolo[3,4-b]pyridin-5-yl)benzaldehyde (**14**)*

Following the general procedure with 4-formylphenylboronic acid (52 mg, 0.35 mmol) the mixture was refluxed for 12 hours. The crude product was purified by flash chromatography on silica gel (90:10 petroleum ether / ethyl acetate) to afford compound **14** as a brown solid. (88 mg; 82%); mp: 139-141 °C ; IR (neat): ῡ= 3047.86, 2830.12, 1709.19, 1342.29, 1033.54, 12.11, cm^{-1} .^{1}H NMR (400 MHz, $CDCl_3$-d) δ 10.11 (s, 1H), 8.32 (d, J = 8.1 Hz, 2H), 8.01 (d, J = 7.6 Hz, 2H), 7.50 (t, J = 7.6 Hz, 2H), 7.39 (d, J = 7.6 Hz, 2H), 7.29 (d, J = 7.2 Hz, 1H), 2.76 (s, 3H), 2.38 (s, 3H), 2.36 (s, 3H). ^{13}C NMR (101 MHz, Chloroform-d) δ 191.9, 156.6, 150.3, 146.1, 142.9, 140.2 , 139.8 , 135.7, 130.89 , 130.3, 130.1, 129.09 , 125.5, 120.97 , 114.8, 25.4, 16.9, 15.9; HRMS (ESI) calcd *m/z* for $[M + H]^+$ $C_{22}H_{20}N_3O$ 342.1528, found 342.1531.

*4.1.13. 3-(3,4,6-Trimethyl-1-phenyl-1H-pyrazolo[3,4-b]pyridin-5-yl)benzonitrile (**15**)*

Following the general procedure with *m*-cyanophenylboronic acid (51 mg, 0.35 mmol) the mixture was refluxed for 12 hours. The crude product was purified by flash chromatography on silica gel (90:10 petroleum ether / ethyl acetate) to afford compound **15** as a yellow solid. (80 mg; 75%); mp: 151-153 °C, IR (neat): ῡ= 3027.76, 2921.11, 2225.34, 1463.21, 1262.45, 1019.66, 817.62, 764.23, 697.81 cm^{-1}. ^{1}H NMR (400 MHz, $CDCl_3$-*d*) δ 8.23 (d, *J* = 8.0 Hz, 2H), 7.65 (d, *J* = 7.7 Hz, 1H), 7.53 (t, *J* = 7.7 Hz, 1H), 7.42 (dd, *J* = 8.2, 7.0 Hz, 4H), 7.19 (t, *J* = 7.4 Hz, 1H), 2.67 (s, 3H), 2.28 (s, 3H), 2.26 (s, 3H). ^{13}C NMR (101 MHz, $CDCl_3$-*d*) δ 156.8, 150.27 , 142.9, 140.8, 140.6, 139.7, 134.68 , 133.6, 131.3, 129.1 , 128.9 , 125.5, 120.8 , 118.7 , 114.8 , 113.3 , 25.4, 16.9, 15.9; HRMS (ESI) calcd *m/z* for $[M + H]^+$ $C_{22}H_{19}N_4$ 339.1531, found 339.1535.

*4.1.14. 3,4,6-Trimethyl-1-phenyl-5-(thiophen-2-yl)-1H-pyrazolo[3,4-b]pyridine (**16**)*

Following the general procedure with 2-thienylboronic acid (40 mg, 0.35 mmol) the mixture was refluxed for 12 hours. The crude product was purified by flash chromatography on silica gel (90:10 petroleum ether / ethyl acetate) to afford compound **16** as a yellow solid. (75 mg; 74%); mp: 161-163 °C, IR (neat): ῡ= 3033.11, 2945.65, 1511.45, 661.23 cm^{-1}, ^{1}H NMR (400 MHz, $CDCl_3$-*d*) δ 8.31 (d, *J* = 8.1 Hz, 2H), 7.54 – 7.43 (m, 3H), 7.24 (t, *J* = 7.3 Hz, 1H), 7.10 (s, 1H), 6.96 (d, *J* = 4.8 Hz, 1H), 2.74 (s, 3H), 2.42 (s, 3H), 2.41 (s, 3H). ^{13}C NMR (101 MHz, $CDCl_3$-d) δ 158.2, 150.1, 142.8, 141.5, 139.9, 138.8, 129.3, 129.1,126.3, 126.1, 125.3, 123.7, 120.9, 115.0, 25.2, 16.8, 15.9; HRMS (ESI) calcd *m/z* for $[M + H]^+$ $C_{19}H_{18}N_3S$ 320.1143, found 320.1141.

*4.1.15. 5-(6-Fluoropyridin-3-yl)-3,4,6-trimethyl-1-phenyl-1H-pyrazolo[3,4-b]pyridine (**17**)*

Following the general procedure with 6-fluoro-3-pyridinylboronic acid (49 mg, 0.35 mmol) the mixture was refluxed for 12 hours. The crude product was purified by flash chromatography on silica gel (90:10 petroleum ether / ethyl acetate) to afford compound **17** as a white solid. (75 mg; 71%); mp: 193-195 °C; IR (neat): ῡ= 3093.09, 2946.65, 1323.38, 1121.98, 1065.12, 842.11, 780.83 cm^{-1}.. ^{1}H NMR (400 MHz, $CDCl_3$-d) δ 8.33 (d, *J* = 8.1 Hz, 2H), 8.11 (s, 1H), 7.68 (dd, *J* = 8.0 Hz, 1H), 7.52 (dd, *J* = 7.4 Hz, 2H), 7.30 (dd, *J* = 8.1 Hz, 1H), 7.10 (d, *J* = 8.3 Hz, 1H), 2.78 (s, 3H), 2.42 (s, 3H), 2.39 (s, 3H) ^{13}C NMR (101 MHz, $CDCl_3$-d) δ 164.4, 157.4, 150.4, 148.6 (d, $^{1}J_{C\text{-}F}$= 14.5 Hz), 142.9, 142.8, 141.4, 139.7, 132.8, 129.1, 125.6, 121.0, 114.9, 109.9 (d, $^{2}J_{CHAr\text{-}F}$ = 37.5 Hz), 25.5, 17.0, 15.9; HRMS (ESI) calcd *m/z* for $[M + H]^+$ $C_{20}H_{18}FN_4$ 333.1437, found 333.1439.

*4.1.16. 5-(4-Chlorophenyl)-3,4,6-trimethyl-1-phenyl-1H-pyrazolo[3,4-b]pyridine (**18**)*

Following the general procedure with 4-chlorophenylboronic acid (49 mg, 0.35 mmol) the mixture was refluxed for 12 hours. The crude product was purified by flash chromatography on silica gel (90:10 petroleum ether / ethyl acetate) to afford compound **18** as a yellow solid. (100 mg; 91%); mp: 147-149 °C; IR (neat): ῡ= 3018.90, 2922.23, 1610.11, 1522.76, 1349.32, 1227.98, 1201.19, 763.42, 681.59 cm^{-1}. ^{1}H NMR (400 MHz, $CDCl_3$-d) δ 8.34 (d, *J* = 8.1 Hz, 2H), 7.51 (dd, *J* = 9.0, 8.1 Hz, 4H), 7.29 (d, *J* = 6.7 Hz, 1H), 7.16 (d, *J* = 7.8 Hz, 2H), 2.77 (s, 3H), 2.40 (s, 3H), 2.39 (s, 3H) ; ^{13}C NMR (101 MHz, $CDCl_3$-d) δ 157.3, 149.9, 142.9, 140.6, 139.8, 137.7, 133.6, 131.4 , 130.1, 129.2, 129.1, 125.4, 121.0, 114.9, 25.4, 16.9, 15.9; HRMS (ESI) calcd *m/z* for $[M + H]^+$ $C_{21}H_{19}ClN_3$ 348.1189, found 348.1193.

Table 2. Screening Suzuki reaction conditions with 4-tolylboronic acid

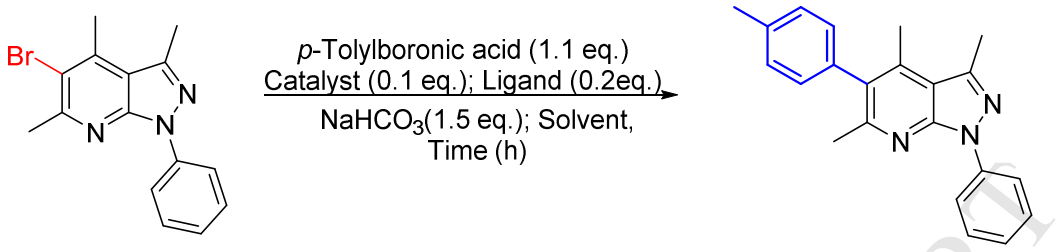

4 **8**

Entry	Catalyst	Ligand	Base	Solvent	Time [h]	Heating system	Conv[%][a]	Yield[%] [b]
1	$Pd(PPh_3)_4$	-	$NaHCO_3$	Toluene /EtOH(2/1)	24	Reflux	100	81
2	$Pd(OAc)_2$	Xantphos	$NaHCO_3$	Toluene /EtOH(2/1)	24	Reflux	71	55
3	$Pd(PPh_3)_4$	-	$NaHCO_3$	1,4-Dioxane	24	Reflux	83	72
4	$Pd(OAc)_2$	Xantphos	$NaHCO_3$	1,4-Dioxane	24	Reflux	64	52
5	$Pd(PPh_3)_4$	-	$NaHCO_3$	Toluene /EtOH(2/1)	12	Reflux	100	98
6	$Pd(PPh_3)_4$	-	$NaHCO_3$	Toluene	24	Reflux	62	49
7	$Pd(OAc)_2$	Xantphos	$NaHCO_3$	Toluene	24	Reflux	39	25
8	**$Pd(PPh_3)_4$ (5%)**	**-**	**$NaHCO_3$**	**Toluene /EtOH(2/1)**	**12**	**Reflux**	**100**	**98**

[a] ^{1}H NMR ratio based on the integration between the CH_3 in the starting material and final product. [b] Isolated yield after column chromatography

4.2. Biological Methods

4.2.1. Cell Culture and Treatments

The human neuroblastoma cell line (SH-SY5Y) used in this study was purchased from the American Type Culture Collection (ATCC, Catalog #CRL-2266). Cells were suspended in complete Dulbecco's modified Eagle Medium (DMEM) (Life Technologies, Gibco BRL, Grand Island, NY) supplemented with 10% fetal bovine serum (FBS, Hyclone), 1% penicillin and streptomycin (100 U/ml, Invitrogen) and plated in cell culture dishes. The cultures were maintained at 37°C in 5% CO_2 95% humidified atmosphere. After reaching 85% confluence, cells were transferred to 96-well plates or culture dish. For MTT experiments, cells were seeded into 96-well cell culture plates at a density of 2x 10^3 cells per well and allowed to adhere for 24 h. The culture medium was then replaced with either fresh medium containing compounds and/or 1-methyl-4-phenylpyridinium ion (MPP^+, 0.1-10 mM) and incubated in 5% CO_2 incubator for 12, 24, 36 or 48 h. Meanwhile, compounds in various concentrations (5, 10, 20 µM) dissolved in dimethyl sulfoxide (DMSO) were added and incubated at 37°C in 5% CO_2 for 3, 6 and 24 hours for cell proliferation assay. For protein analysis, cells were seeded into 6-well cell culture plates at a density of 5 x 10^5 cells/well and allowed to adhere to

the surface for 24 h. The culture medium was then replaced with either fresh medium containing MPP+ (2 mM) or **8**, **10, 13**, **14**, **16**, **18** at two different concentrations (1 and 5 µM) for 12 h. When used, all compounds were added 1 h prior to MPP^+ exposure.

4.2.2. Cell viability assessment by MTT assay

Percent cell viability was assessed using the 3-(4,5-dimethylthiazol-2-yl)-2,5-diphenyl tetrazolium bromide (MTT) assay. Briefly, following exposures, MTT (in final concentration 0.5 mg/ml) was added to each well, and plates were incubated for 3 h at 37°C in 5% CO_2 humidified incubator. The reaction mixture was carefully removed and 200 µl DMSO was added to each well. The plate was shaken at room temperature for 1 h and then the absorbance was measured at 570 nm and 630 nm using a microplate reader (VersaMax, Molecular Devices, USA). Percent survival was plotted relative to vehicle control cells, which were normalized to 100% survival.

4.2.3. Isolation of proteins and Western blotting

The cells were washed with PBS and lysed with an ice-cold lysis buffer (10 mM Tris pH 7.4, 150 mM NaCl, 1% NP-40, 0.5% sodium deoxycholate, 0.1% SDS, 1 mM EDTA, 1 mM Na_3VO_4, 10 mM NaF, 100 µg/ml PMSF, 1 µg/ml aprotinin, 4 µg/ml leupeptin), followed by centrifugation at 14 000×g for 15 min at +4°C. Western blotting was performed by loading 10 µg protein on 10% (w/v) tris-glycine denaturing gels and separating proteins by electrophoresis, then transferring to PVDF membrane. After blocking, the membrane was incubated with primary antibodies, anti-bax rabbit monoclonal antibody (1:1000, Cell Signaling Technology) or anti-Bcl-2 rabbit monoclonal antibody (1:1000, Cell Signaling Technology) or anti-Bcl-xl rabbit monoclonal antibody (1:1000, Cell Signaling Technology) or anti-caspase-3 rabbit monoclonal antibody (1:1000, Cell Signaling Technology) at +4°C over night. Following the incubation, the membrane was incubated with anti-β-actin mouse monoclonal antibody (1:1000, Cell Signaling Technology) at RT for 1h. After washing, the membrane was incubated with HRP-conjugated goat polyclonal anti-rabbit IgG (1:2000, Cell Signaling Technology) as the secondary antibody for 2 hours at room temperature and then incubated for 5 min with SuperSignal West Pico Chemiluminescent Substrate (Thermo Scientific). The signal intensities were visualized by the Fusion. FX imaging system (Vilber Lourmat).

4.2.4. Statistical analysis

Data were expressed as means ± standard deviation (SD) for five independent experiments in triplicate. Comparisons of means between groups were performed by one-way

analysis of variance (ANOVA) followed by Tukey's post hoc test. $p < 0.05$ was considered statistically significant.

Supporting Information. ^{1}H and ^{13}C NMR spectra of compounds.

References

[1] R.N. Misra, D.B. Rawlins, H. Xiao, W. Shan, I. Bursuker, K.A. Kellar, J.G. Mulheron, J.S. Sack, J.S. Tokarski, S.D. Kimball, K.R. Webster, 1*H*-Pyrazolo[3,4-*b*]pyridine inhibitors of cyclin-dependent kinases, Bioorg. Med. Chem. Lett. 13 (2003) 1133-1136.

[2] R.N. Misra, H. Xiao, D.B. Rawlins, W. Shan, K.A. Kellar, J.G. Mulheron, J.S. Sack, J.S. Tokarski, S.D. Kimball, K.R. Webster, 1*H*-Pyrazolo[3,4-*b*]pyridine inhibitors of cyclin-dependent kinases: highly potent 2,6-difluorophenacyl analogues, Bioorg. Med. Chem. Lett. 13 (2003) 2405-240.

[3] L. Meijer, M. Flajolet, P. Greengard, Pharmacological inhibitors of glycogen synthase kinase 3, Trends in Pharm. Sci. 25 (2004) 471-480.

[4] I. Sekikawa, J. Nishie, S. Tono-oka, Y. Tanaka, S. Kakimoto, Antituberculous compounds. XXVIII. Synthesis of pyrazolopyridines, J. Heterocycl. Chem. 10 (1973) 931-932.

[5] H. Foks, D. Pancechowska-Ksepko, A. Kvdzia, Z. Zwolska, M. Janowiec, E. Augustynowicz-Kopec, Synthesis and antibacterial activity of 1*H*-pyrazolo[3,4-*b*]pyrazine and -pyridine derivatives, Il Farmaco 60 (2005) 513-517.

[6] F.E. Goda, A.A.M. Abdel-Aziz, O.A. Attef, Synthesis, antimicrobial activity and conformational analysis of novel substituted pyridines: BF_3-promoted reaction of hydrazine with 2-alkoxy pyridines, Bioorg. Med. Chem. 12 (2004) 1845-1852.

[7] D.S. Kundariya, B.M. Bheshdadia, N.K. Joshi, P.K. Patel, Synthesis, characterization and pharmacological evaluation of some novel Schiff bases containing 1*H*-pyrazolo[3,4-b]pyridine moiety, Int. J. Chem. Tech. Res. 3 (2011) 238-243.

[8] J. Witherington, V. Bordas, A. Gaiba, N.S. Garton, A. Naylor, A.D. Rawlings, B.P. Slingsby, D.G. Smith, A.K. Takle, R.W. Ward, 6-Aryl-pyrazolo[3,4-b]pyridines: potent inhibitors of glycogen synthase kinase-3 (GSK-3), Bioorg. Med. Chem. Lett. 13 (2003) 3055-3057.

[9] J. Witherington, V. Bordas, S.L. Garland, D.M.B. Hickey, R.J. Ife, J. Liddle, M. Saunders, D.G. Smith, R.W. Ward, 5-Aryl-pyrazolo[3,4-b]pyridines: potent inhibitors of glycogen synthase kinase-3 (GSK-3), Bioorg. Med. Chem. Lett. 13 (2003) 1577-1580.

[10] A. Straub, J.P. Stasch, C. Alonso-Alija, J. Benet-Buchholz, B. Ducke, A. Feurer, C. Fürstner, NO-independent stimulators of soluble guanylate cyclase, Bioorg. Med. Chem. Lett. 11 (2001) 781-784.

[11] D.J. Sanger, H. Depoortee, The Pharmacology and Mechanism of action of zolpidem, CNS Drug Rev. 4, (1998), 323-340.

[12] H. Mohler, F. Crestani, U. Rudolph, GABA(A)-receptor subtypes: a new pharmacology, Curr. Opin. Pharmacol. 1 (2001) 22-25.

[13] L. Jasmin, S.D. Rabkin, A. Granato, A. Boudah, P.T. Ohara, Analgesia and hyperalgesia from GABA-mediated modulation of the cerebral cortex, Nature 424 (2003) 316-320.

[14] S.A. Thompson, P.B. Wingrove, L. Connelly, P.J. Whiting, K.A. Wafford, Molecular dissection of benzodiazepine binding and allosteric coupling using chimeric γ-aminobutyric acidA receptor subunits, Molecular Pharmacology 61 (2002) 861-869.

[15] W.P. Blackaby, J.R. Atack, F. Bromidge, R. Lewis, M.G.N. Russell, A. Smith, K. Wafford, R.M. McKernan, L.J. Street, J.L. Castro, Pyrazolopyridinones as functionally selective GABAA ligands, Bioorg. Med. Chem. Lett. 15 (2005) 4998-5002.

[16] M. P. Mattson, Apoptosis in neurodegenerative disorders, Nature Review Molecular Cell Biology 1, (2000) 120–129.

[17] E. Radi, P. Formichi, C. Battisti, A. Federico, Apoptosis and oxidative stress in neurodegenerative diseases, Journal of Alzheimer's, Disease (2014) 125-52.

[18] S. Przedborski, M. Vila, The 1-methyl-4-phenyl-1,2,3,6-tetrahydropyridine mouse model: a tool to explore the pathogenesis of Parkinson's disease, Ann. N. Y. Acad. Sci. 991 (2003) 189-198.

[19] O. Rascol, P. Payoux, F. Ory, J.J. Ferreira, C. Brefel-Courbon, J.L. Montastruc, Limitations of current Parkinson's disease therapy, Ann Neurol. 53 (2003) Suppl 3:S3-12; discussion S12-5.

[20] H.D. Foster, A. Hoffer. Two faces of L-DOPA : benefits and adverse side effects in the treatment of encephalitis lethargica, Parkinson’s disease, multiple sclerosis and amyotrophic lateral sclerosis, Med Hypotheses, 62 (2) (2004) 177-181.

[21] D. Merims, N. Giladi, Dopamine dysregulation syndrome, addiction and behavioral changes in Parkinson’s disease, Parkinsonism Relat Disord. 14(4) (2008) 273-280.

[22] S. Fadel, F. Suzenet, A. Hafid, E.M. Rakib, M. Khouili, M.D. Pujol, G. Guillaumet, Synthesis of new compounds containing the pyrazolo[3,4-*b*]pyridine-3-one subunit, J. Heterocycles. Chem. 46 (2009) 1177-1184.

[23] S. Fadel, S. Hamri, Y. Hajbi, F. Suzenet, A. Hafid, E.M. Rakib, M. Khouili, M.D. Pujol, G. Guillaumet, Synthesis of new pyrazolo[3,4-*b*]pyridin-3-ones and pyrazolo[1,5-*a*]pyrimidin-2(1*H*)-one and study of the pyrazolic nitrogen reactivity, ARKIVOC (ii) (2011) 240-251.

[24] S. Przedborski, V. Jackson-Lewis, Mechanisms of MPTP toxicity, Mov. Disord. 13 (1998) Suppl. 1, 35-38.

[25] T.P. Singer, R.R. Ramsay, Mechanism of the neurotoxicity of MPTP, FEBS Lett. 274 (1990) 1-8.

[26] D.Y. Lee, K.S. LeE, H.J. Lee, Y.H. Noh, D.H. Kim, J.Y. Lee, S.H. Cho, O.J. Yoon, W.B. Lee, K.Y. Kim, Y.H. Chung, S.S. Kim, Kynurenic acid attenuates MPP(+)-induced dopaminergic neuronal cell death via a Bax-mediated mitochondrial pathway, Eur J Cell Biol. 87 (2008) 389-397.

[27] C.P. Fall, J.P. Jr. Bennett, Characterization and time course of MPP+ -induced apoptosis in human SH-SY5Y neuroblastoma cells, J Neurosci Res. 55(5) (1999) 620-628.

[28] J. Yang, X. Liu, K. Bhalla, C.N. Kim, A.M. Ibrado, J. Cai, T.I. Peng, D.P. Jones, X. Wang, Science, 275 (1997) 1129-1132.

[29] M. Crompton, Bax, Bid and the permeabilization of the mitochondrial outer membrane in apoptosis, Curr. Opin. Cell. Biol. 12 (2000) 414-419.

[30] D. Blum, S. Torch., N. Lambeng, M. Nissou, A.L. Benabid, R. Sadoul, J.M. Verna, Prog. Neurobiol., 65 (2001) 135-172.

[31] P. Janhom , P. Dharmasaroja, Neuroprotective Effects of Alpha-Mangostin on MPP(+)-Induced Apoptotic Cell Death in Neuroblastoma SH-SY5Y Cells, J Toxicol. (2015) 919058.

[32] G. Tommonaro, N. Garcia-Font, R.M. Vitale, B. Pejin, C. Iodice, S. Canadas, J. Marco-Contelles, M.J. Oset-Gasque, Avarol derivates as competitive AChE inhibitors, non hepatotoxic and neuroprotective agents for Alzheimer's disease, Eur. J. Med Chem, 122 (2016) 326-338.

[33] N. Eleftheriadis, h. Poelman, N. G.J. Leus, B. Honrath, C.G. Neochoritis, A. Dolga, A. Dömling, F.J. Dekker, Design of a novel thiophene inhibitor of 15-lipoxygenase1 with both antiinflammatory and neuroprotective properties, Eur. J. Med Chem, 122 (2016) 786-801.

[34] M. Estrada, C. Herrera-Arozamena, C. Perez, D. Vina, A. Romero, J.A. Morales-Garcia, A. Perez-Castillo, M.I. Rodriguez-Franco. New cinnamic –N-benzylpiperidine and cinnamic –N,N- dibenzyl(N-methyl)amine hybrids as Alzheimer-directed multitarget

drugs with antioxidant, cholinergic, neuroprotective and neurogenic properties, Eur. J. Med Chem, 122 (2016) 376-386.

[35] G. Chen, K.A. Bower, C. Ma, S. Fang, S. C.J. Thiele, J. Luo, Glycogen synthase kinase 3beta (GSK3beta) mediates 6-hydroxydopamine-induced neuronal death, FASEB J. 18 (2004) 1162-1164.

[36] R.L. Jayaraj, K. Tamilselvam, T. Manivasagam, N. Elangovan, Neuroprotective effect of CNB-001, a novel pyrazole derivative of curcumin on biochemical and apoptotic markers against rotenone-induced SK-N-SH cellular model of Parkinson's disease, J. Mol. Neurosci. 51 (2013) 863-870.

LIST OF CAPTIONS

Figure 1. Selected examples of pyrazolopyridine derivatives that can be used for potential therapies in the treatment of serious diseases.

Table 1. Optimization of reaction condensation between **1** and **2**

Table 3. Scope of Suzuki–Miyaura cross coupling of **4**

Figure 2. Evaluation of cell viability of SH-SY5Y cells exposed to various concentrations (0.1-10 mM) of MPP^+ at indicated times. Cells were treated for 12, 24, 36 and 48 h at 37°C. Data represent the mean ± SD of at least six independent experiments in triplicate and are expressed as percentage of control cells.

Figure 3. Effects of newly synthesized compounds on cell viability in MPP^+-induced dopaminergic cell death. All values are means ± SDs (n = 5). * $p<0.05$ significant difference from MPP^+ and 10 or 20 µM concentrations of compound treatments. ** $p<0.05$ significant difference from MPP^+-treated cells.

Table 4. The percentage of neuroprotection-induced by compounds against MPP^+-induced neurotoxicity in SH-SY5Y cells.

Figure 4. The changes in proapoptotic bax protein levels following MPP^+ treatments for 3, 6, 12, 24, 48 h in SH-SY5Y cells. *$p\leq0.05$ significant difference from control group and 3 or 6 hours-treated cells.

Figure 5. The changes in bax, caspase-3, bcl-2 and bcl-xl protein levels following 5 µM **8, 10, 13, 14, 16** or **18** against 2 mM MPP^+-induced apoptosis. Representative Western blots showing protein expression of protein levels following treatments. Graphs indicate the relative densitometric values of indicated proteins. Quantification of protein product was performed by densitometric scanning. Data are normalized by using the β-actin signal and

expressed as arbitrary densitometric units. Values are means ± SD; n = 3 in each group. *p<0.05 significant difference from MPP^+-treated cells.

Figure 6. The changes in bax, caspase-3 and bcl-xl protein levels following 1 μM **8, 10, 13, 14, 16** or **18** against 2 mM MPP^+-induced apoptosis. Representative Western blots showing protein expression of protein levels following treatments. Graphs indicate the relative densitometric values of indicated proteins. Quantification of protein product was performed by densitometric scanning. Data are normalized by using the β-actin signal and expressed as arbitrary densitometric units. Values are means ± SD; n = 3 in each group. *p<0.05 significant difference from MPP^+-treated cells.

Table 2. Screening Suzuki reaction conditions with 4-tolylboronic acid

Highlights

- Heterocyclic compounds based on pyrazolopyridine scaffold have a role on dopaminergic neuroprotection
- Apoptotic pathways are among the targets of compounds in neurodegeneration.

Supporting information

Synthesis of new heterocyclic compounds based on pyrazolopyridine scaffold and evaluation of their neuroprotective potential in MPP^+-induced neurodegeneration

Jabrane Jouha [a,b], Mohammed Loubidi [a], Jamila Bouali [b], Salha Hamri [b], Abderrafia Hafid [b], Franck Suzenet [a], Gérald Guillaumet [a], Taner Dagcı [c], Mostafa Khouili [b], Fadime Aydın Köse[d], Luciano Saso [e], Güliz Armagan [d, *]

[a]Institut de Chimie Organique et Analytique, Université d'Orléans, UMR-CNRS 7311, BP 6759, rue de Chartres, 45067 Orléans cedex 2, France.

[b]Laboratoire de Chimie Organique et Analytique, Université Sultan Moulay Slimane - Faculté des Sciences et Techniques, BP 523, 23000 Beni-Mellal, Morocco.

[c]Department of Physiology and Center for Brain Research, Faculty of Medicine, Ege University, 35100 Bornova, Izmir, Turkey.

[d]Department of Biochemistry, Faculty of Pharmacy, Ege University, 35100 Bornova, Izmir, Turkey.

[e]Department of Physiology and Pharmacology "Vittorio Erspamer", Sapienza University of Rome, P. le Aldo Moro 5, 00185 Rome, Italy.

Corresponding authors:

Güliz Armagan, Department of Biochemistry, Faculty of Pharmacy, Ege University, 35100 Bornova, Izmir, Turkey.

Table of contents

1. ^{1}H and ^{13}C NMR spectra of compounds

3,4,6-Trimethyl-1-phenyl-1H-pyrazolo[3,4-b]pyridine (3).

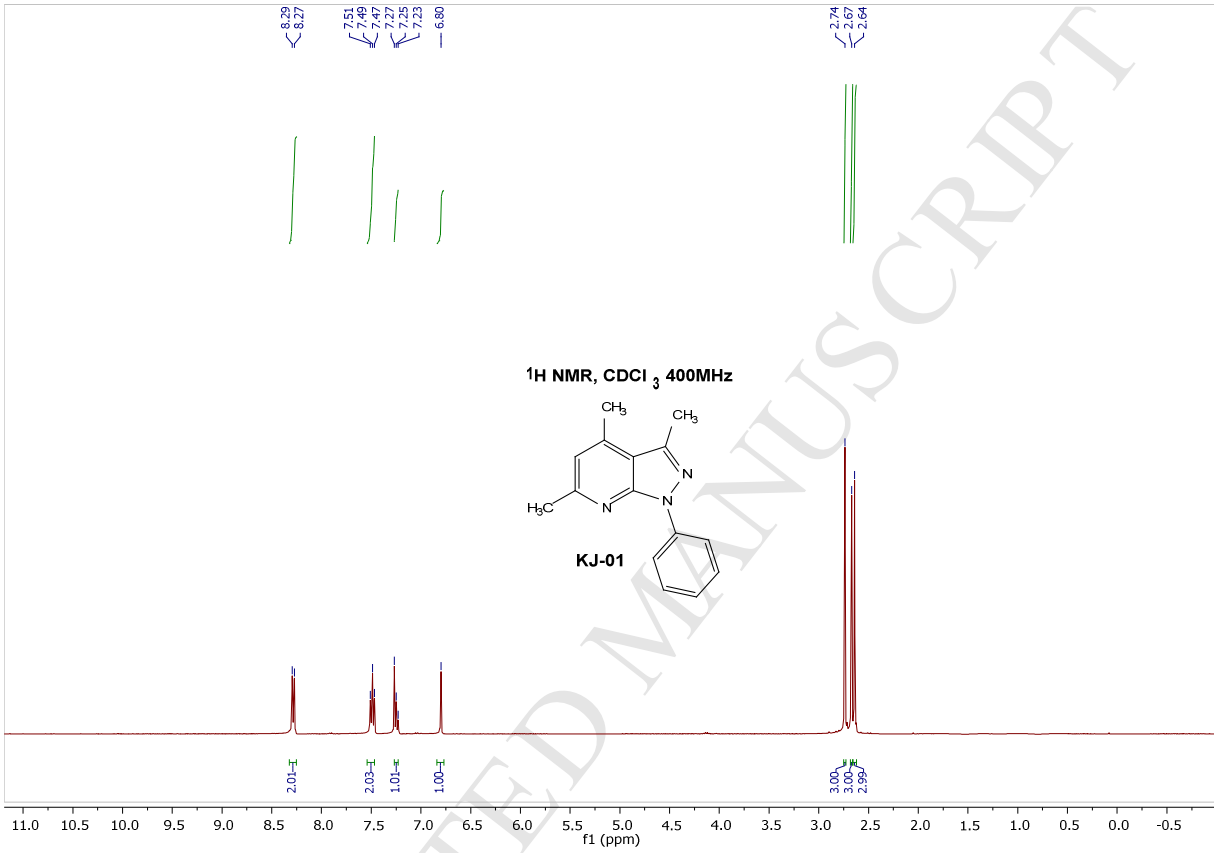

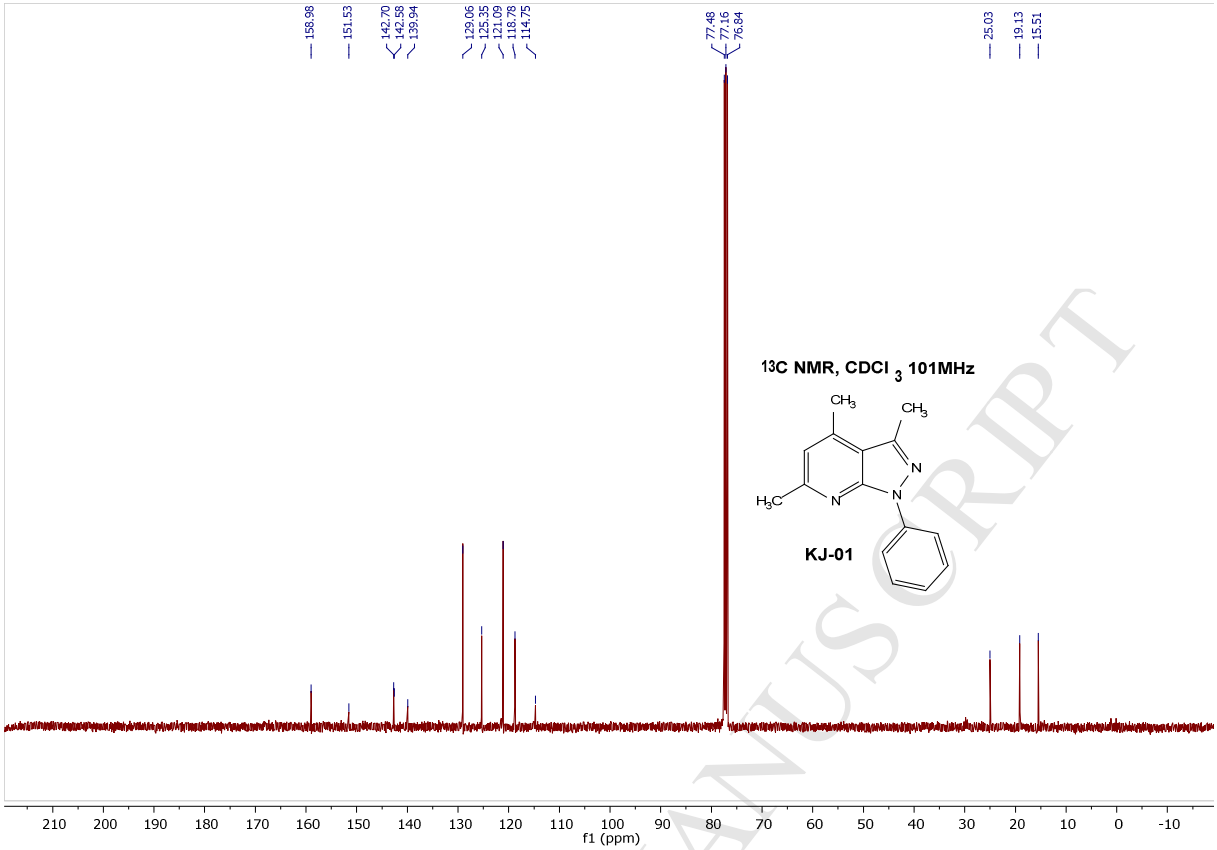

5-bromo-3,4,6-Trimethyl-1-phenyl-1H-pyrazolo[3,4-b]pyridine (4).

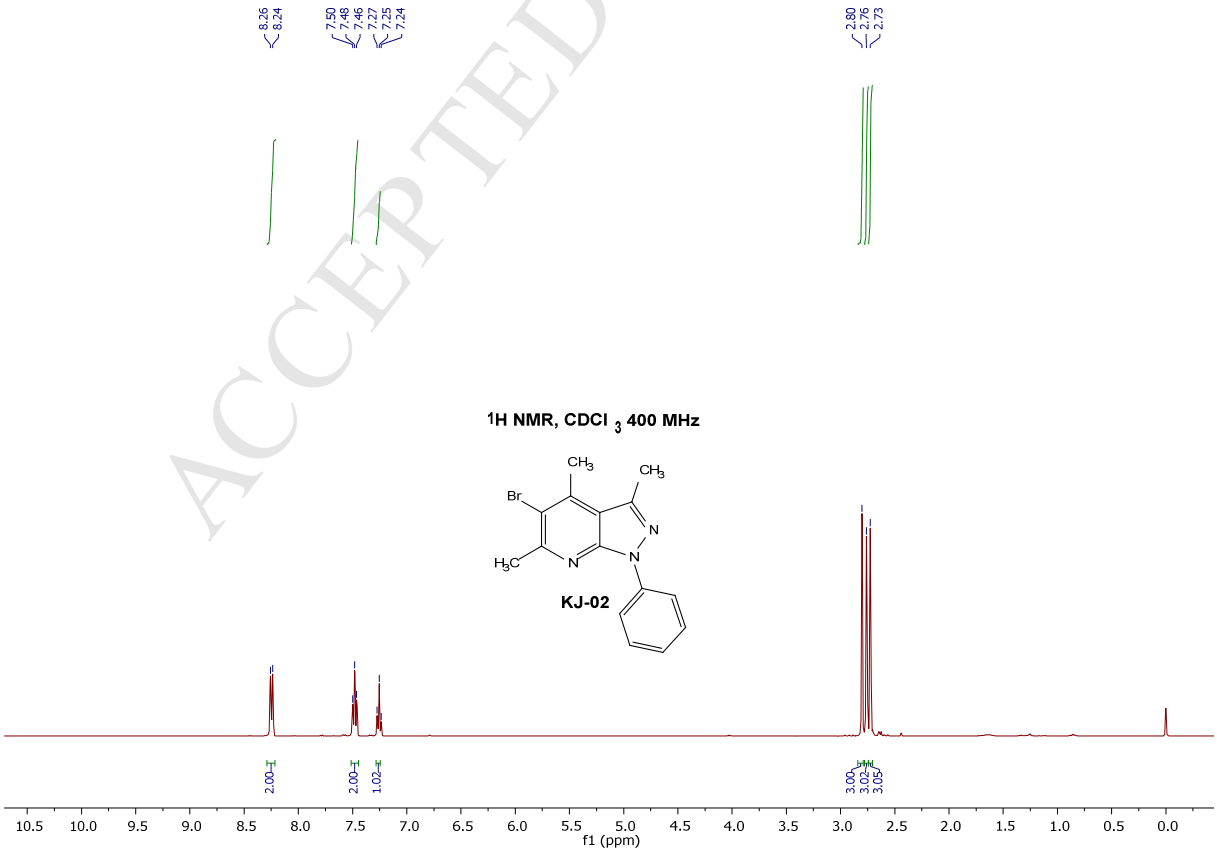

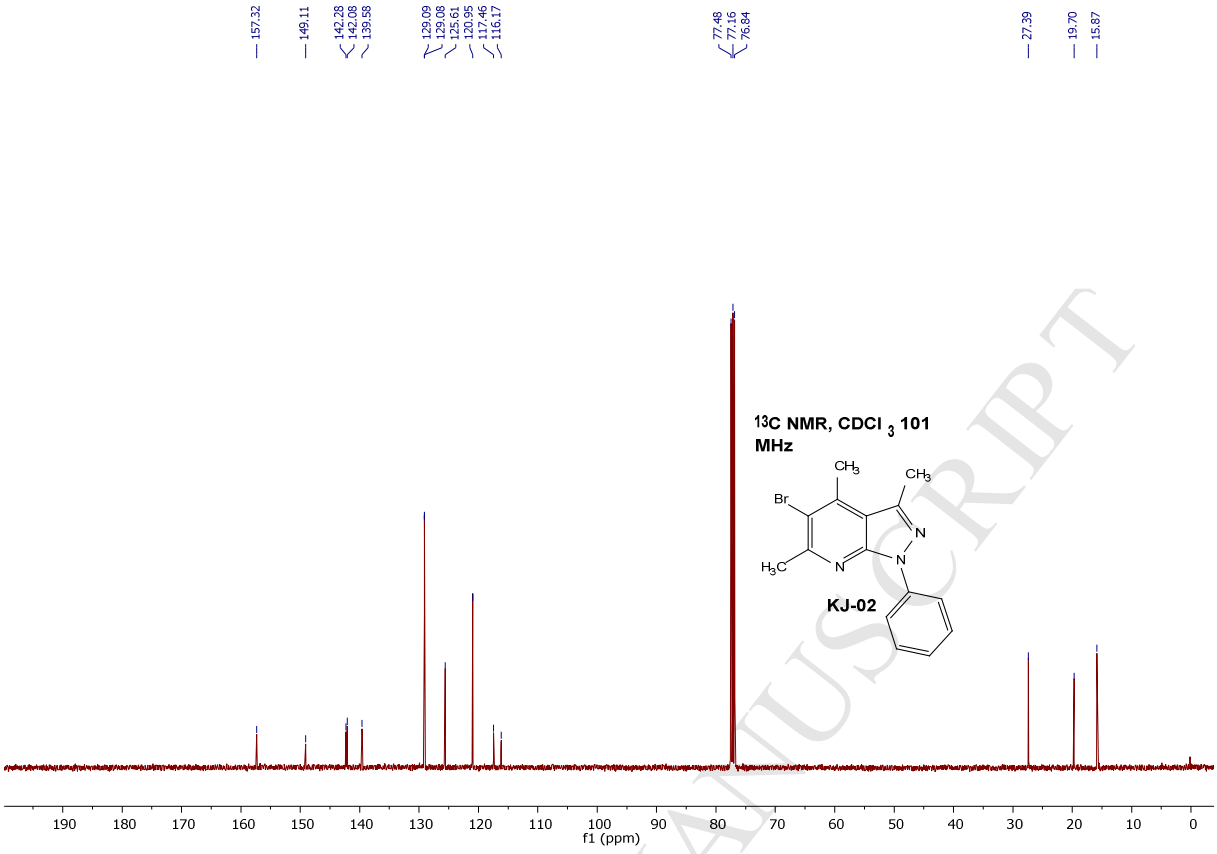

5-(4-Methoxyphenyl)-3,4,6-trimethyl-1-phenyl-1H-pyrazolo[3,4-b]pyridine (5).

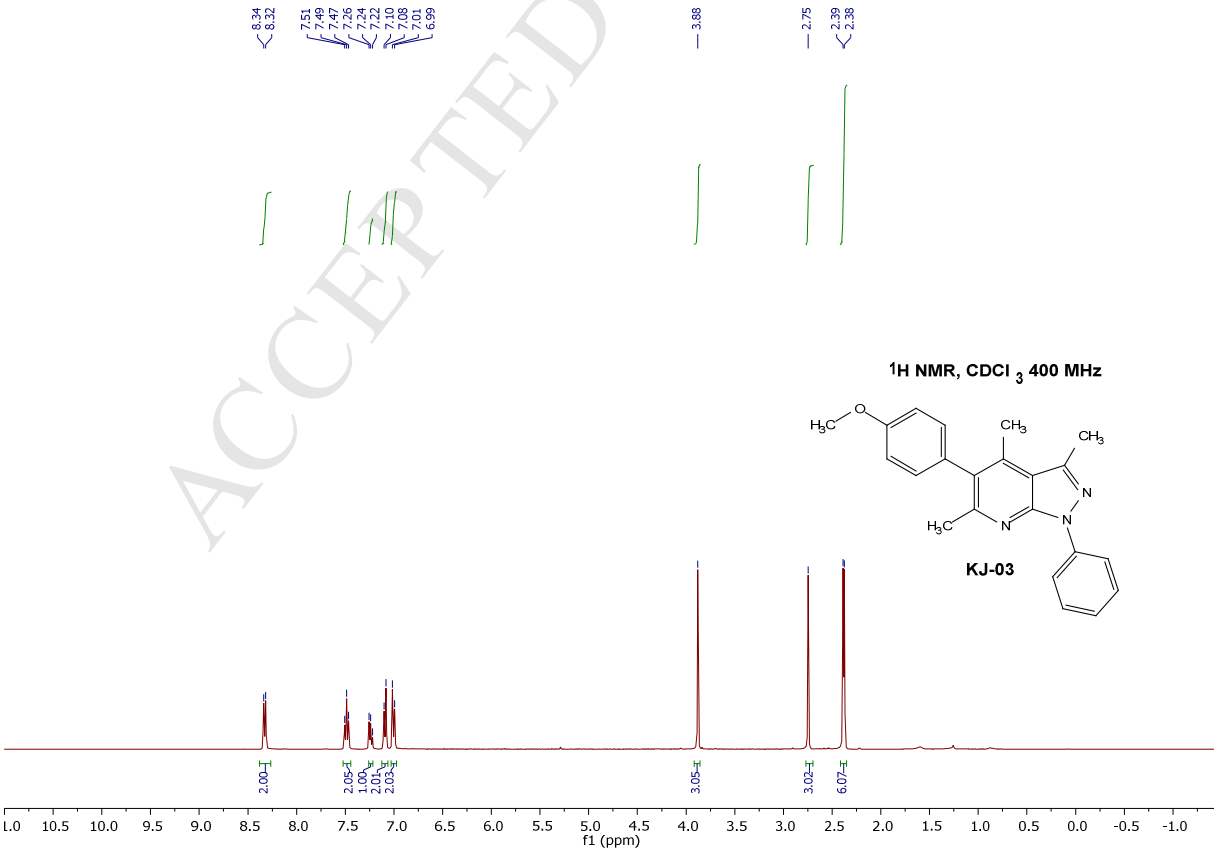

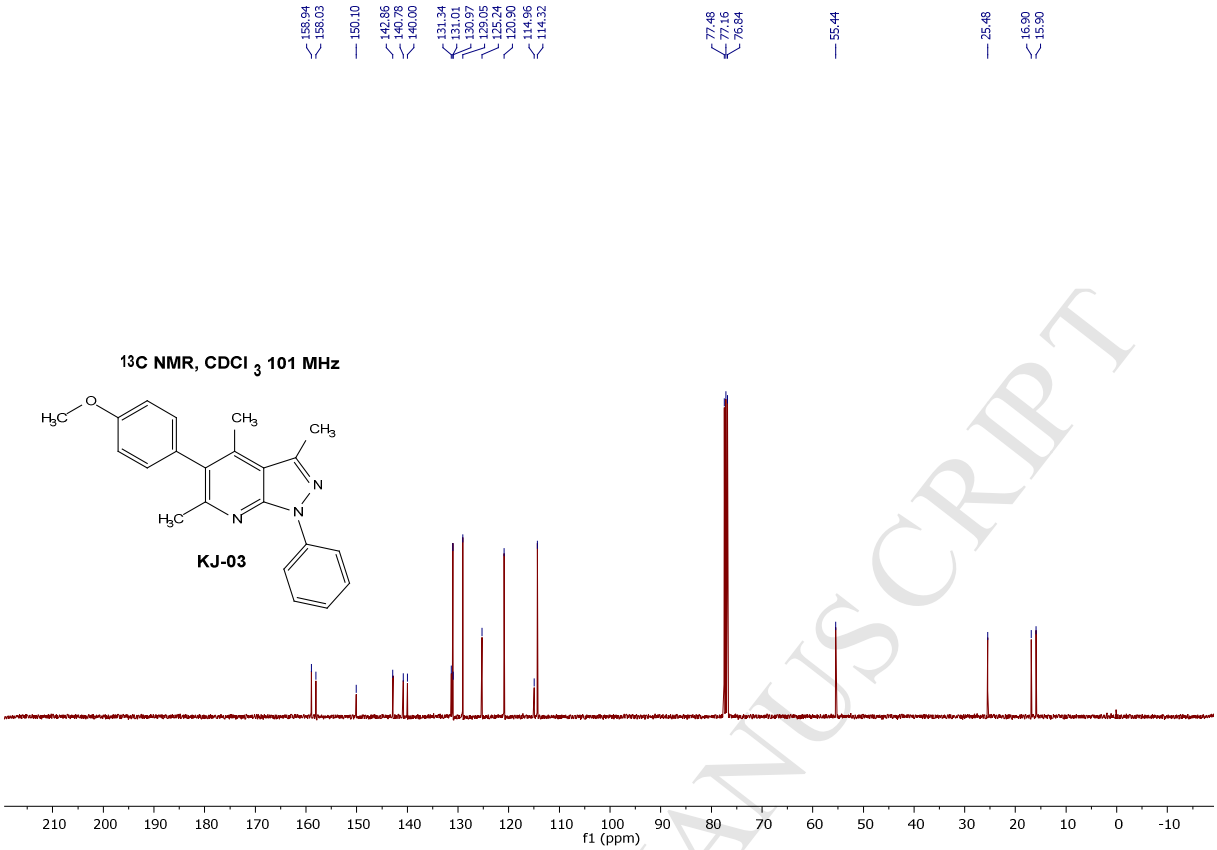

3,4,6-Trimethyl-1-phenyl-5-(o-tolyl)-1H-pyrazolo[3,4-b]pyridine (6).

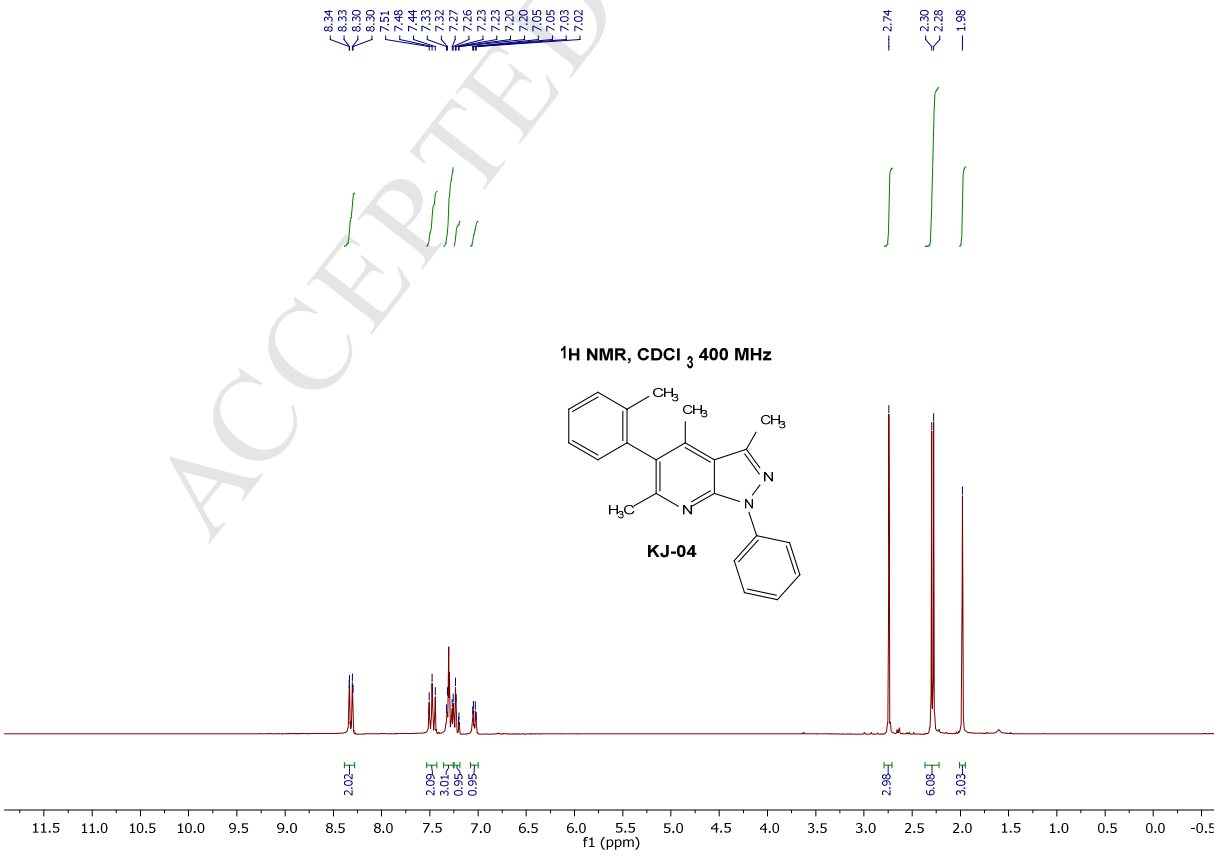

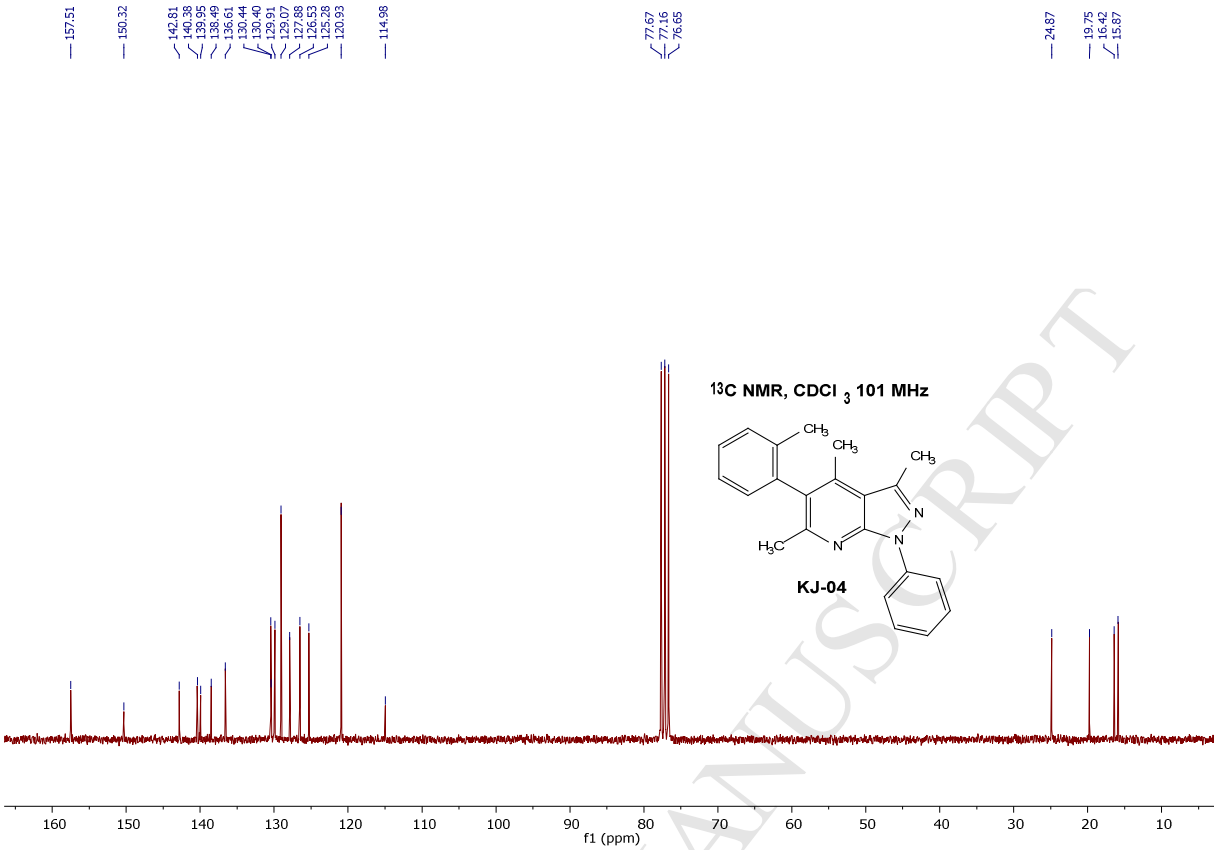

3,4,6-Trimethyl-1-phenyl-5-(m-tolyl)-1H-pyrazolo[3,4-b]pyridine (7).

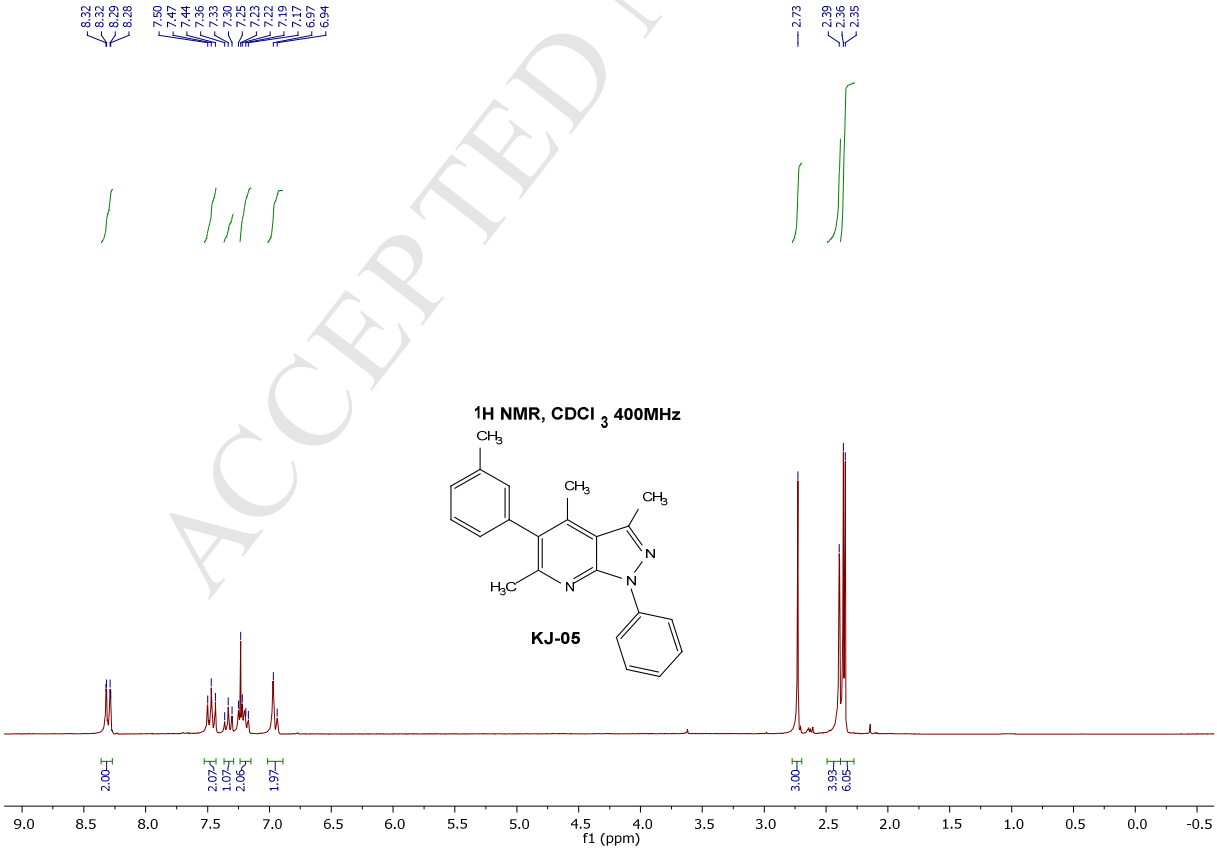

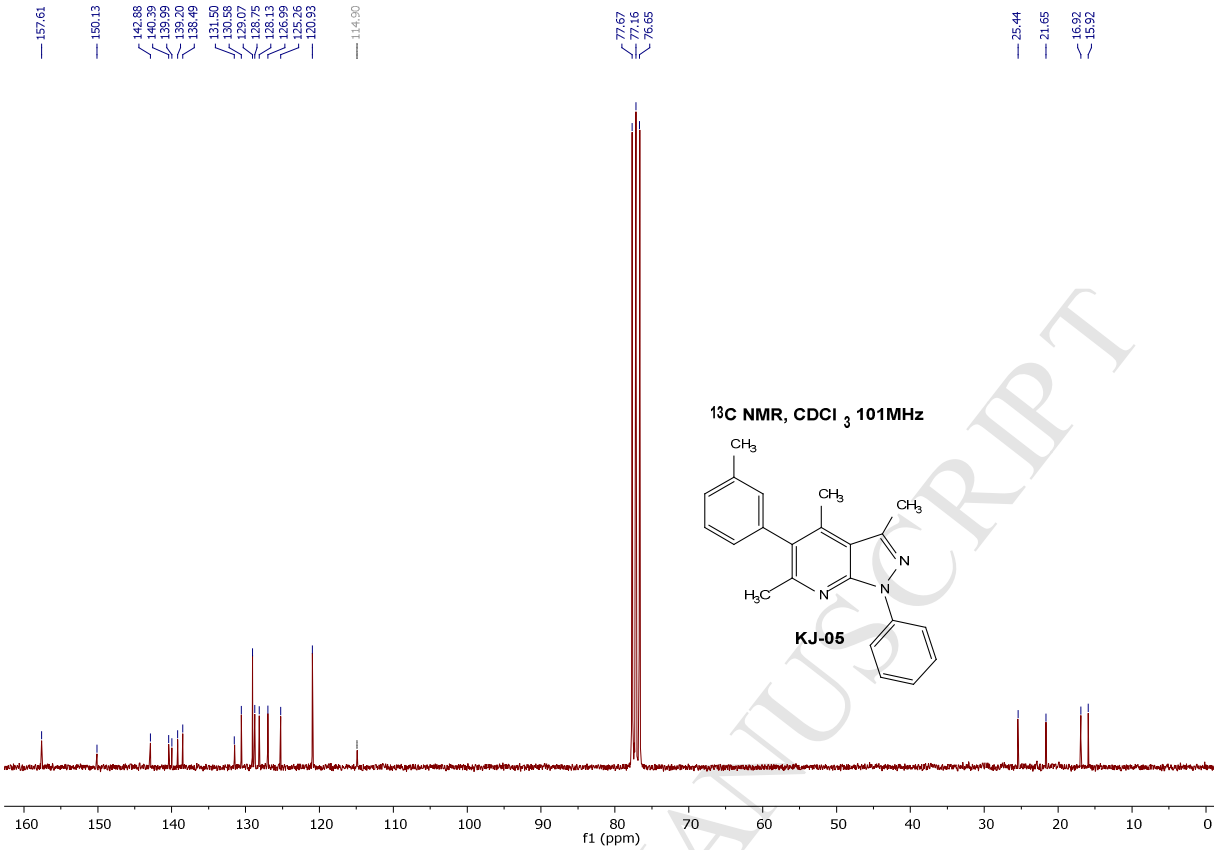

3,4,6-Trimethyl-1-phenyl-5-(p-tolyl)-1H-pyrazolo[3,4-b]pyridine (8).

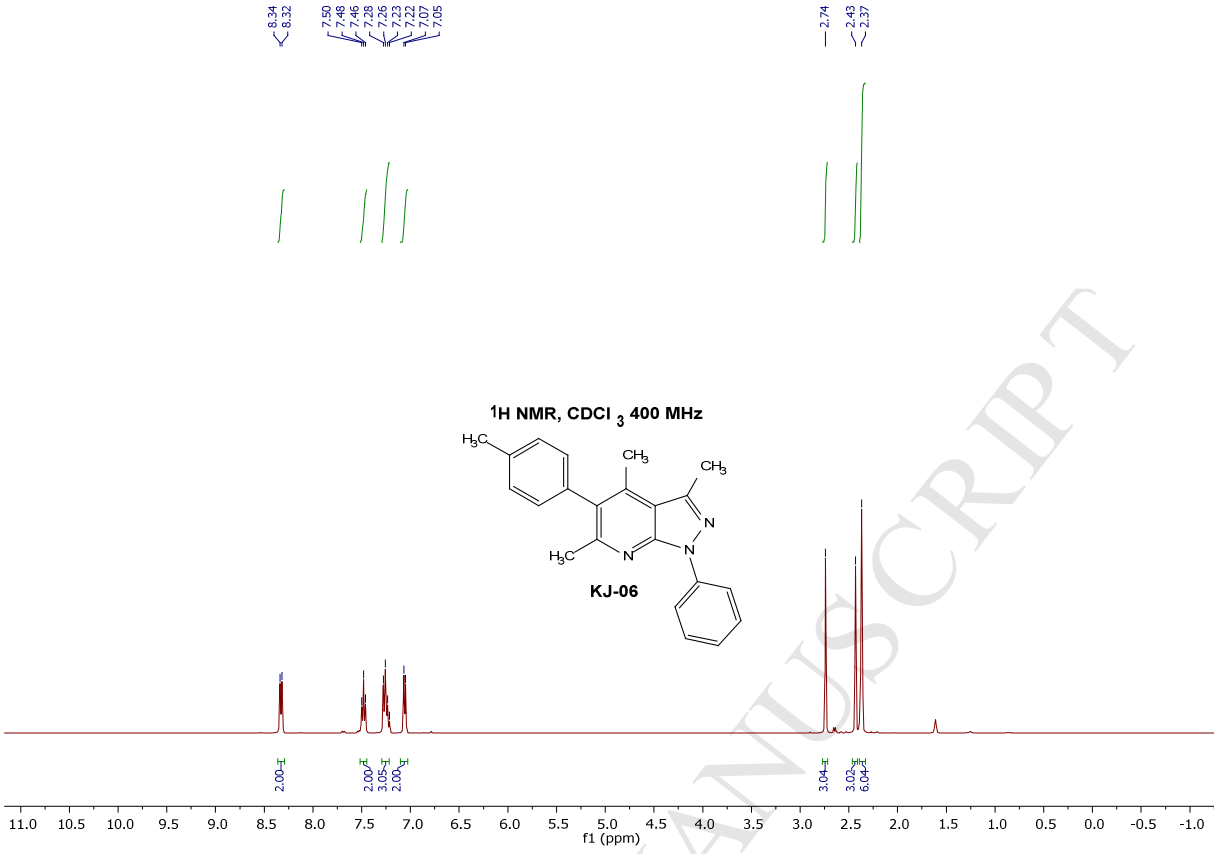

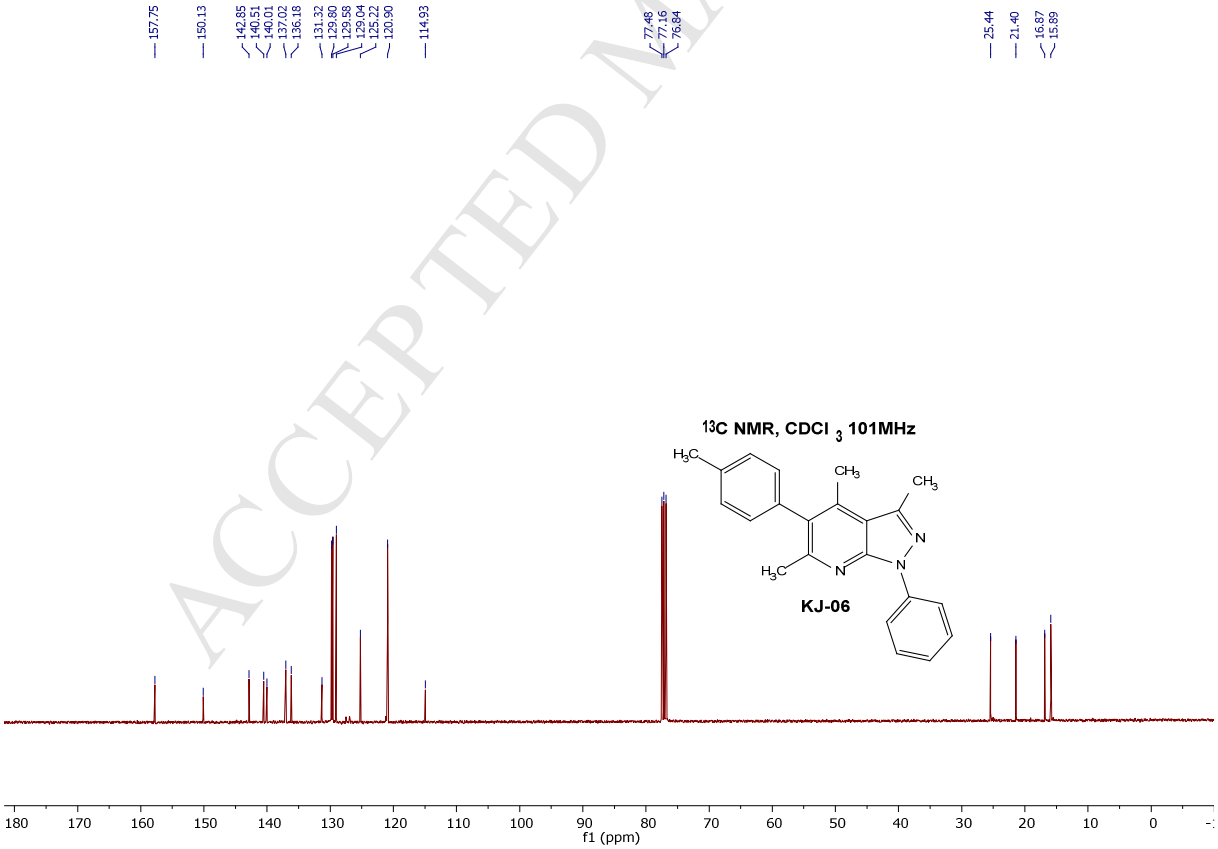

3,4,6-Trimethyl-1,5-diphenyl-1H-pyrazolo[3,4-b]pyridine (9).

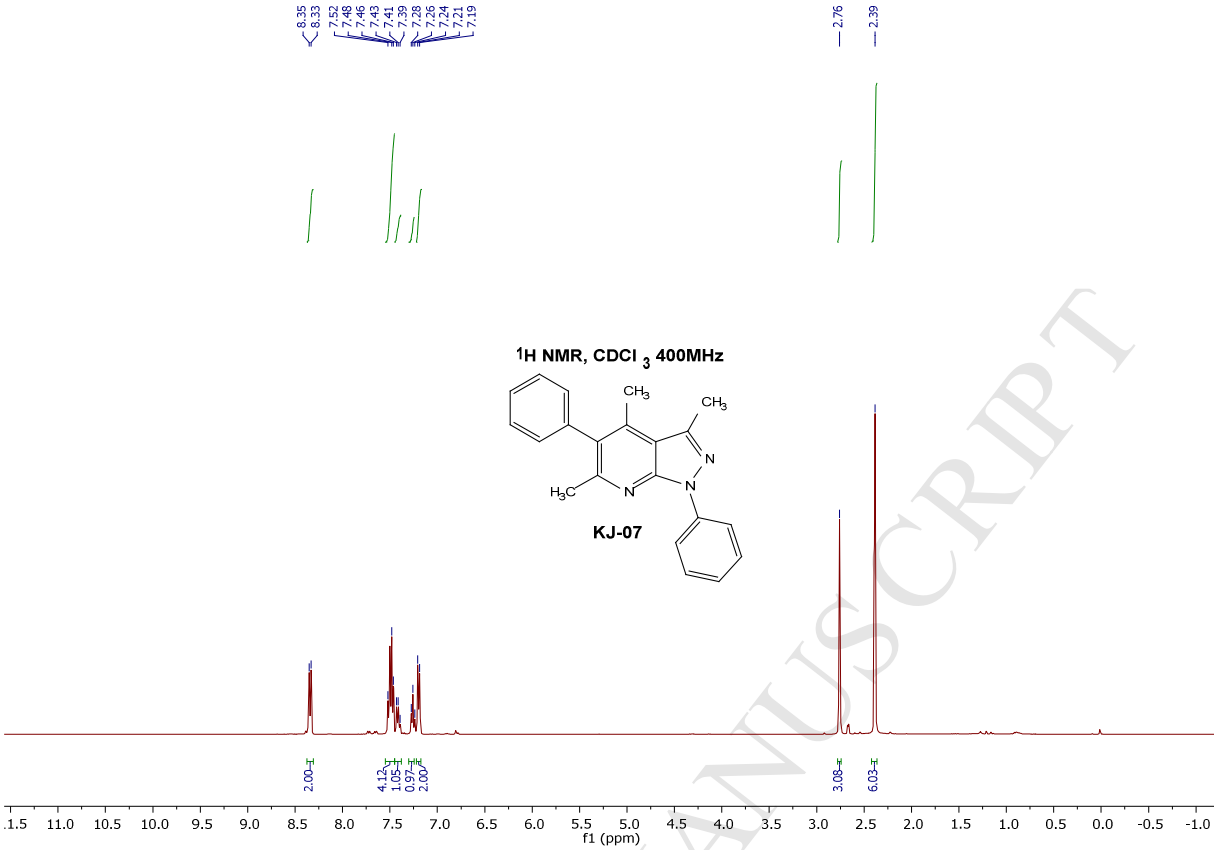

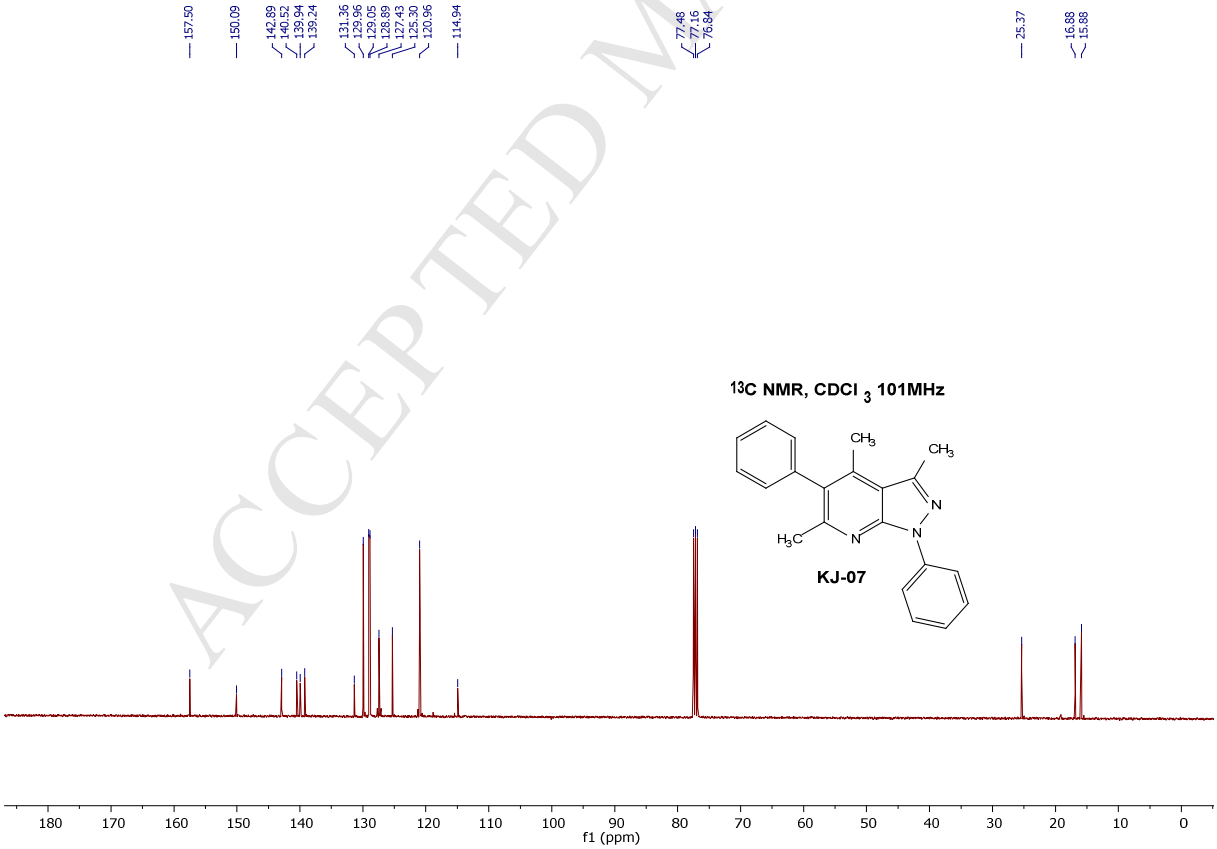

3,4,6-Trimethyl-1-phenyl-5-(4-(trifluoromethyl)phenyl)-1H-pyrazolo[3,4-b]pyridine (10).

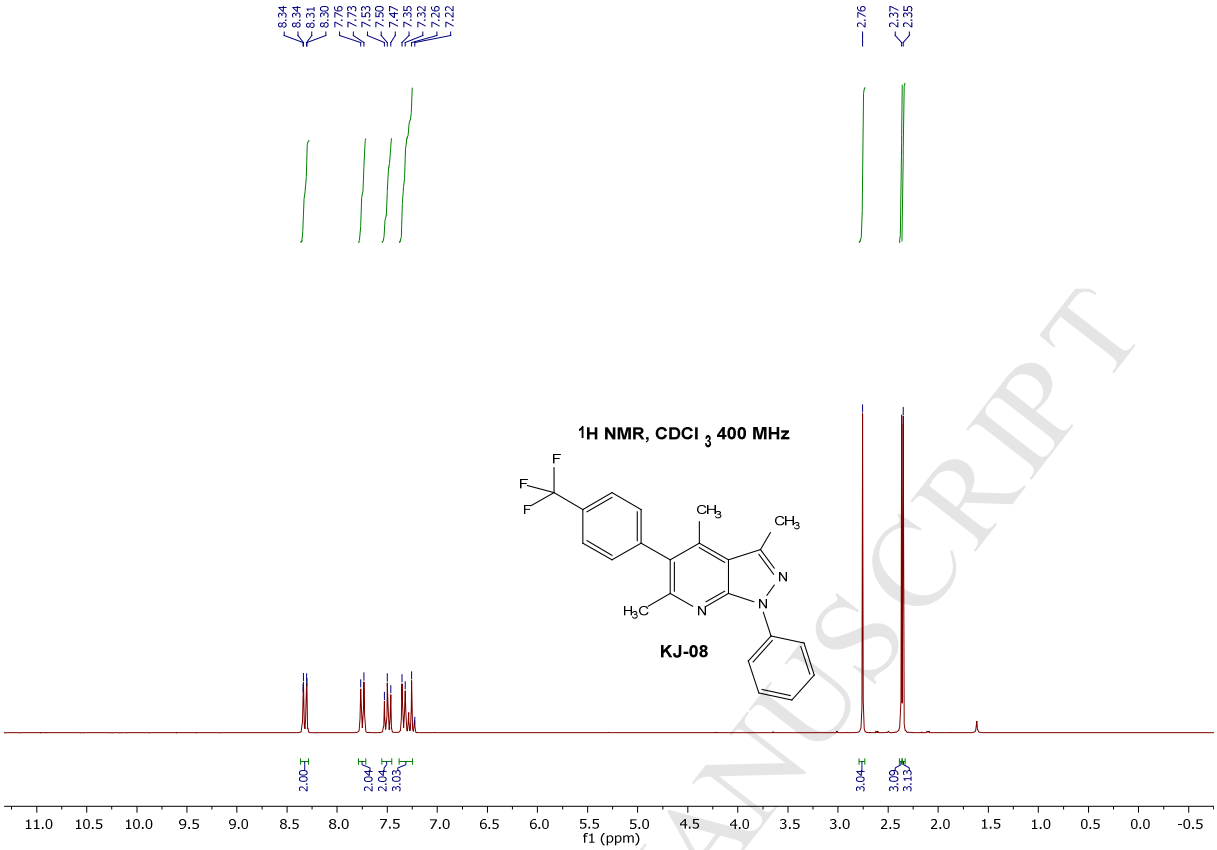

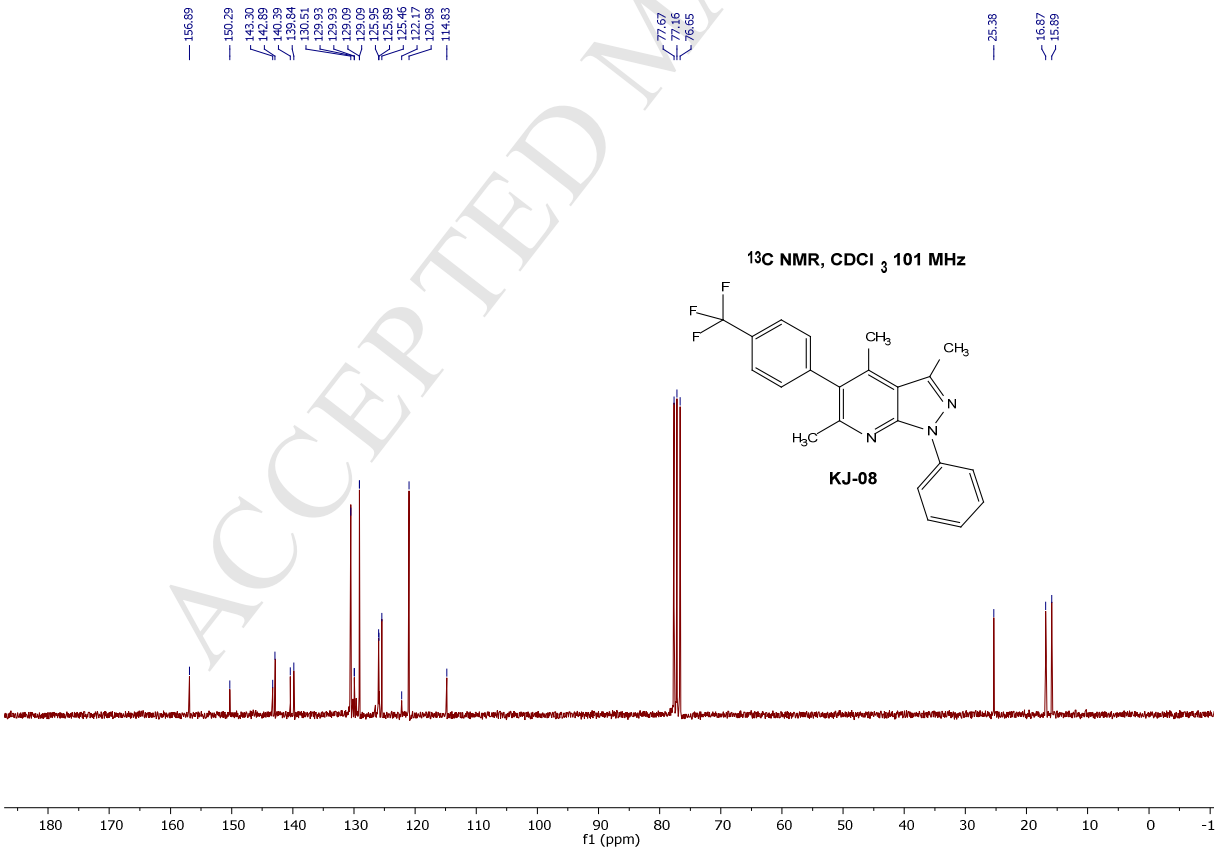

Ethyl-4-(3,4,6-trimethyl-1-phenyl-1H-pyrazolo[3,4-b]pyridin-5-yl)benzoate (11).

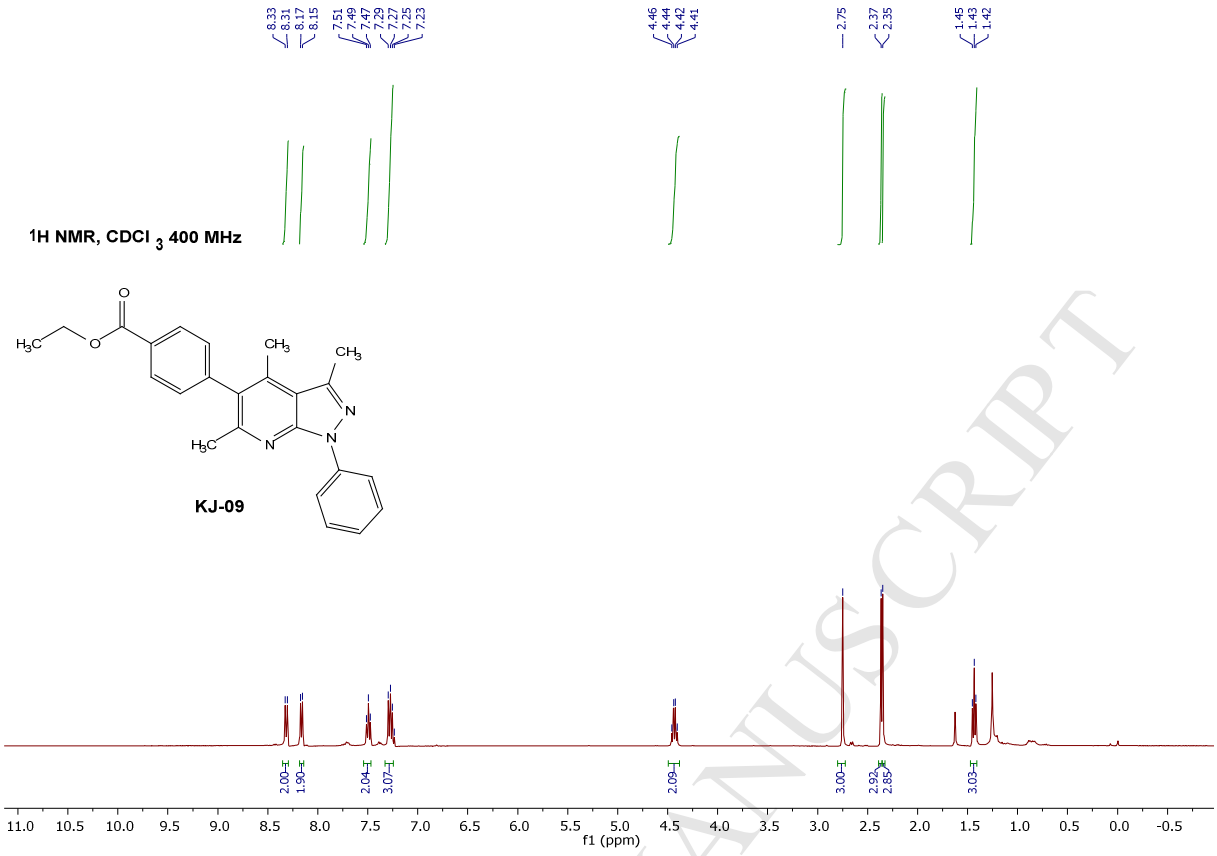

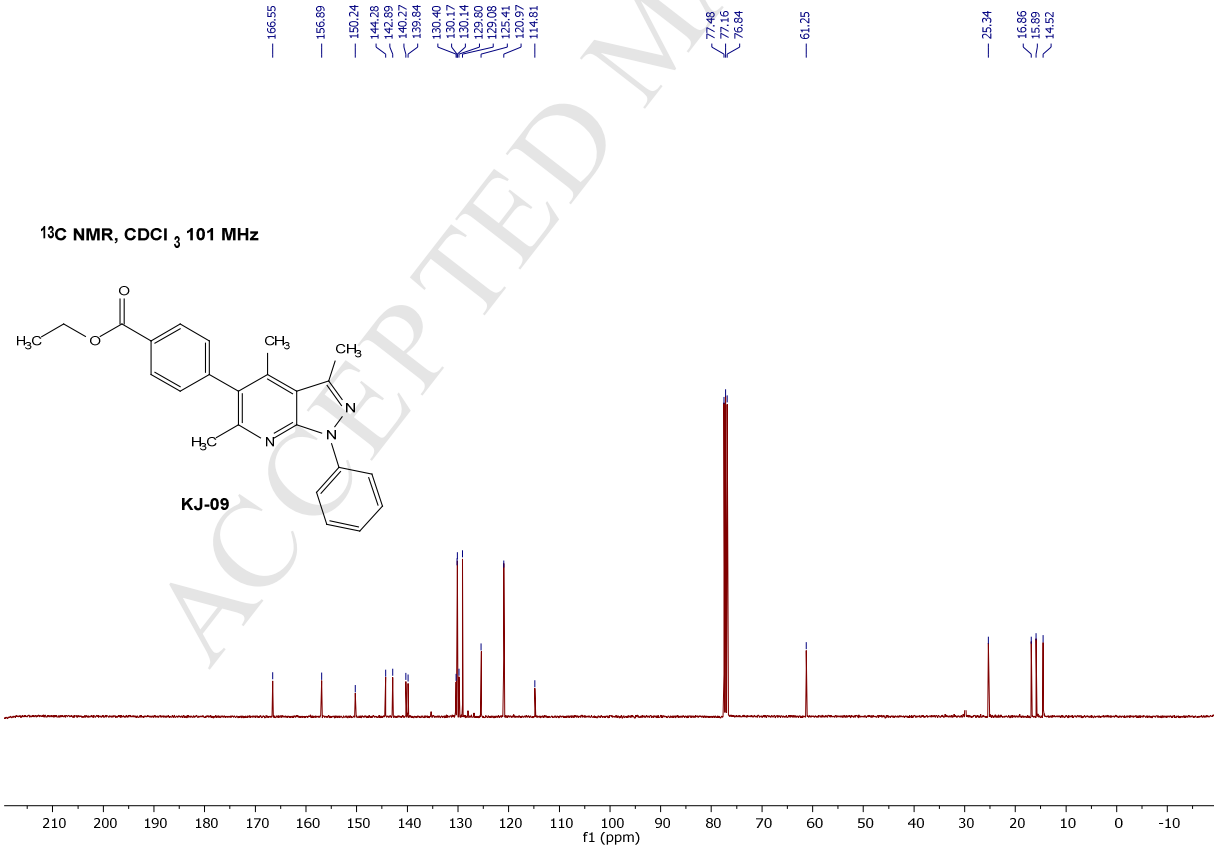

N,N-Dimethyl-4-(3,4,6-trimethyl-1-phenyl-1H-pyrazolo[3,4-b]pyridin-5-yl)aniline (12).

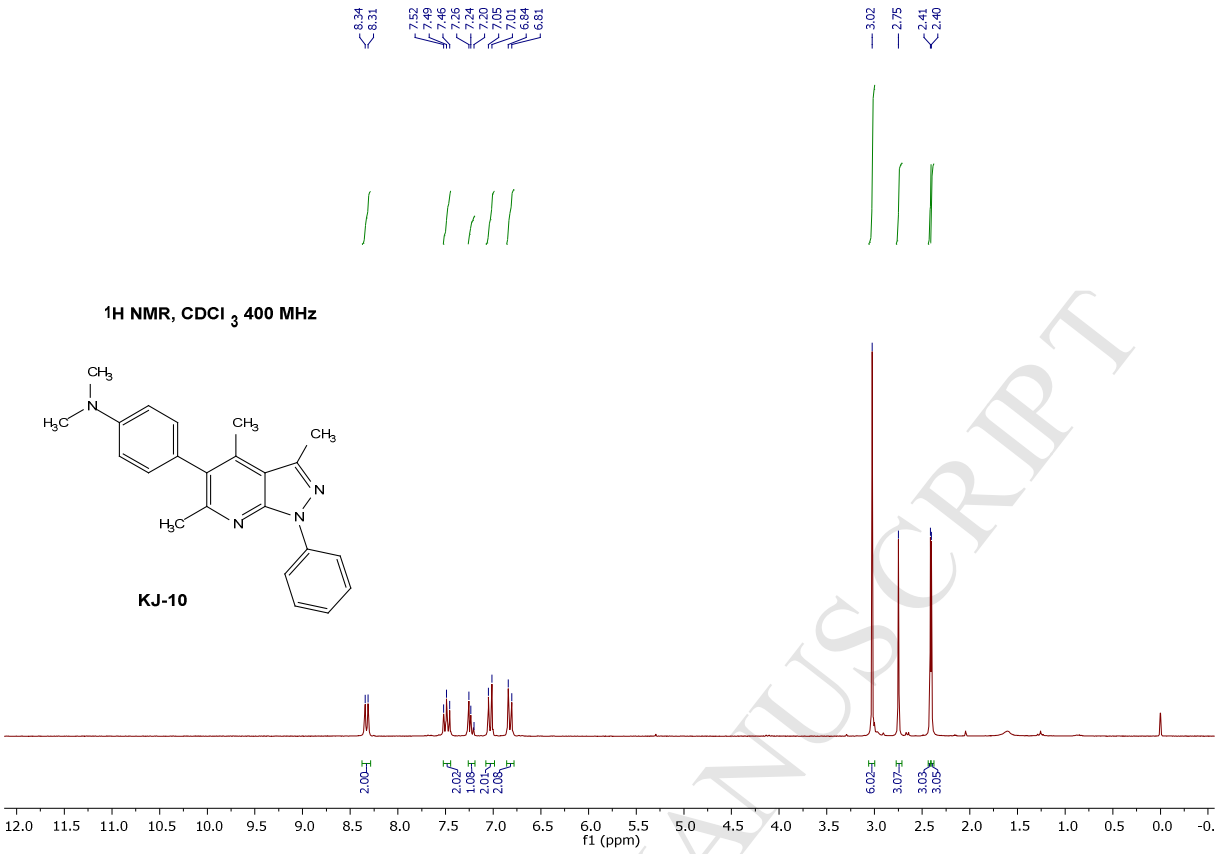

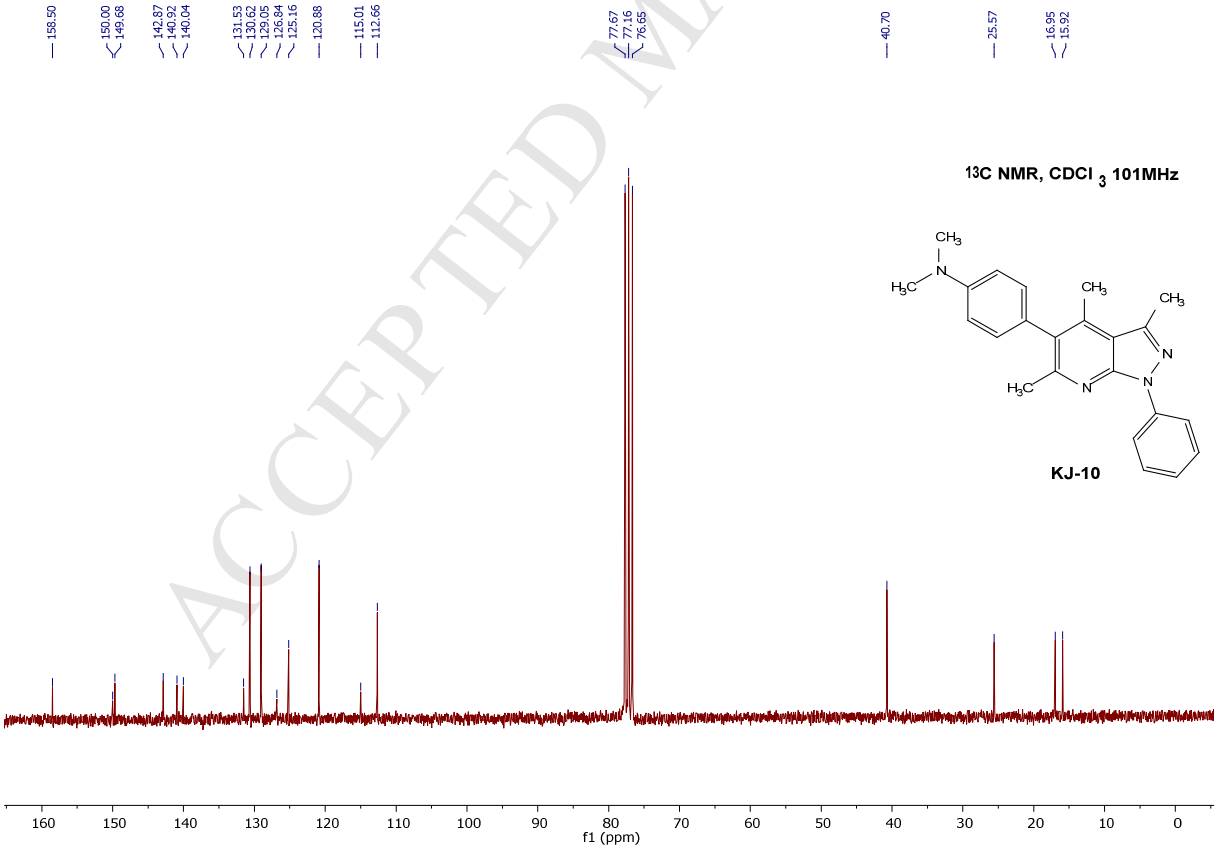

3,4,6-Trimethyl-5-(4-nitrophenyl)-1-phenyl-1H-pyrazolo[3,4-b]pyridine (13).

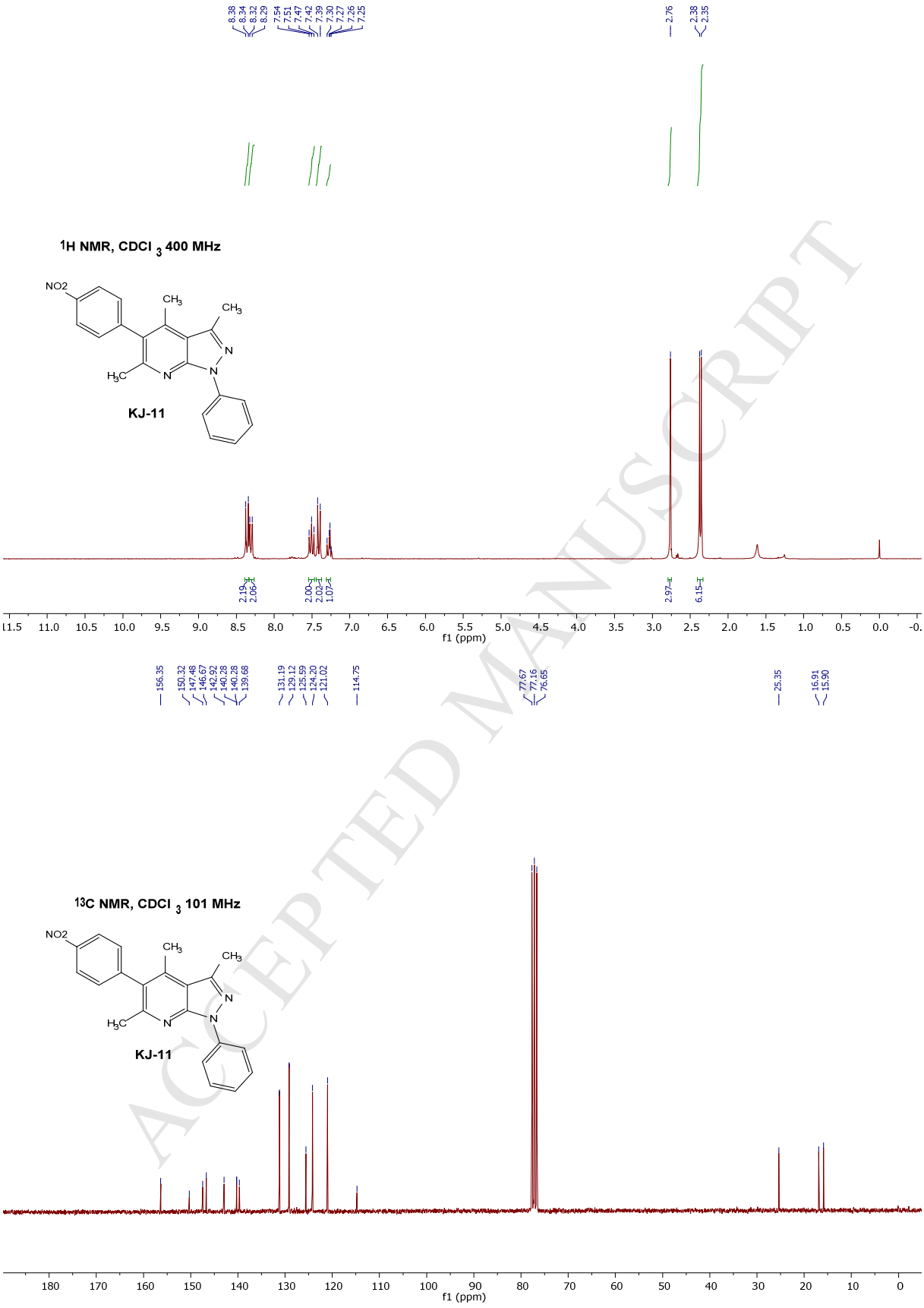

4-(3,4,6-Trimethyl-1-phenyl-1H-pyrazolo[3,4-b]pyridin-5-yl)benzaldehyde (14).

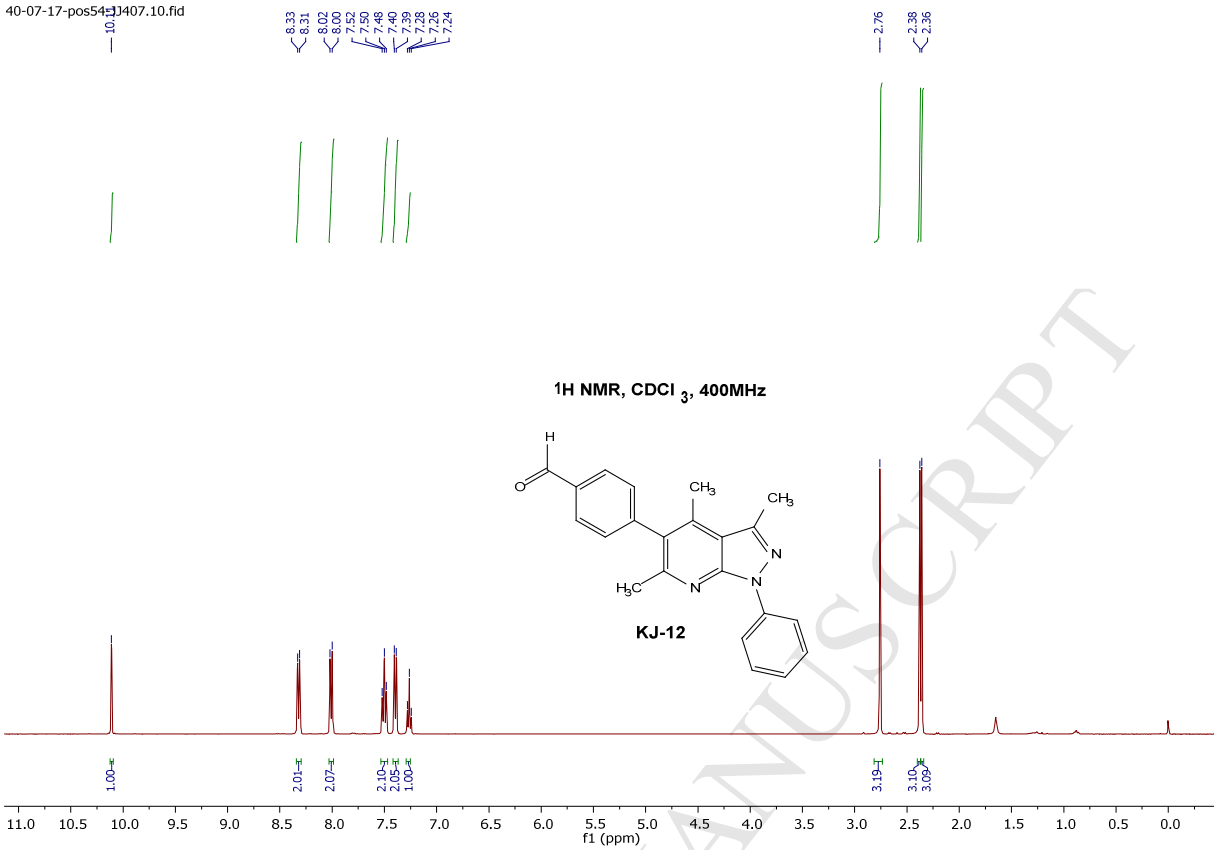

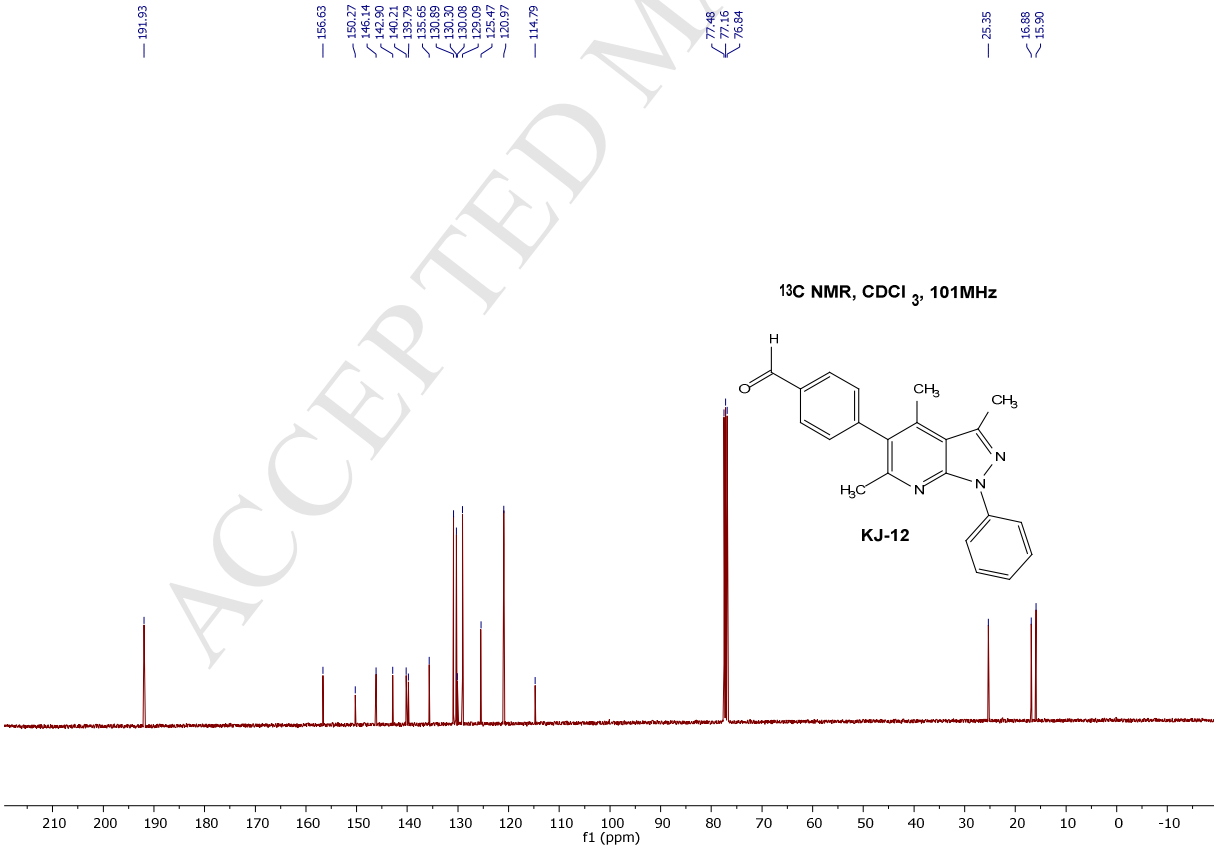

3-(3,4,6-Trimethyl-1-phenyl-1H-pyrazolo[3,4-b]pyridin-5-yl)benzonitrile (15).

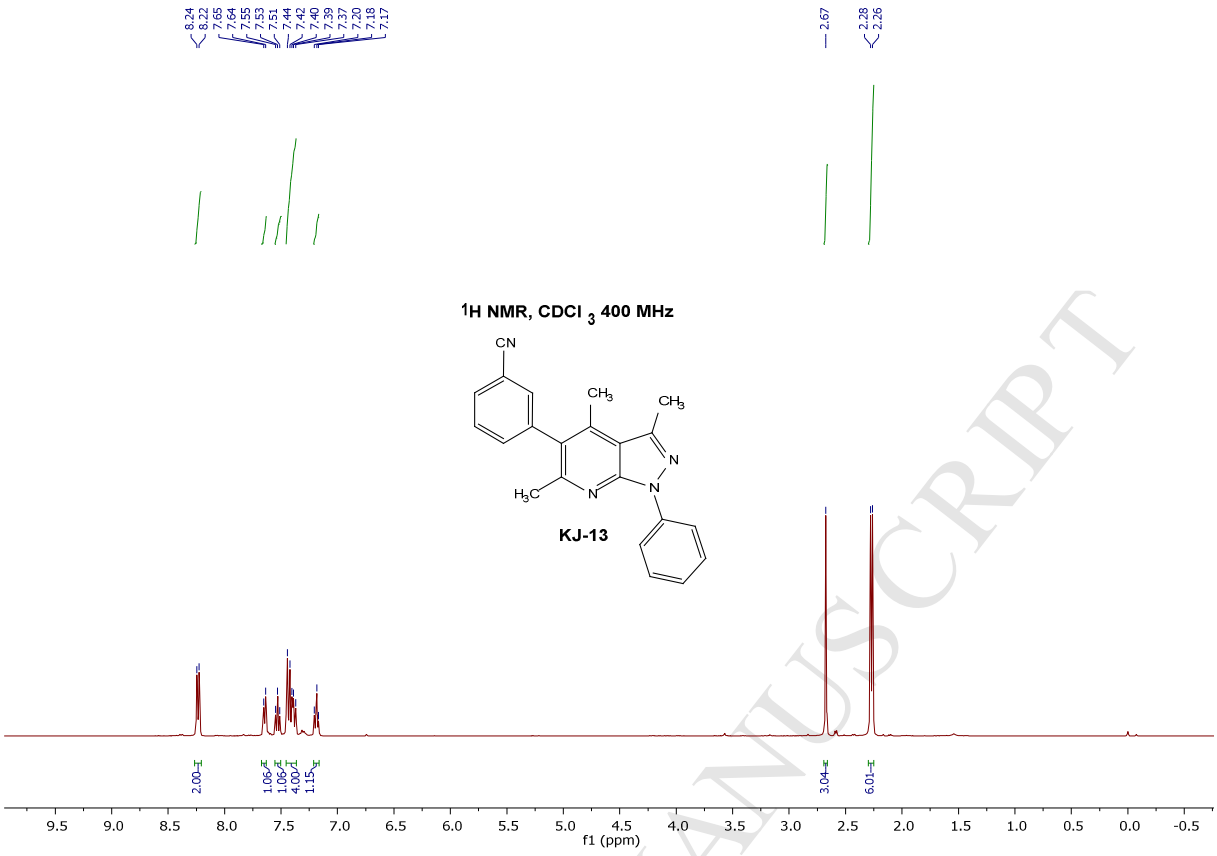

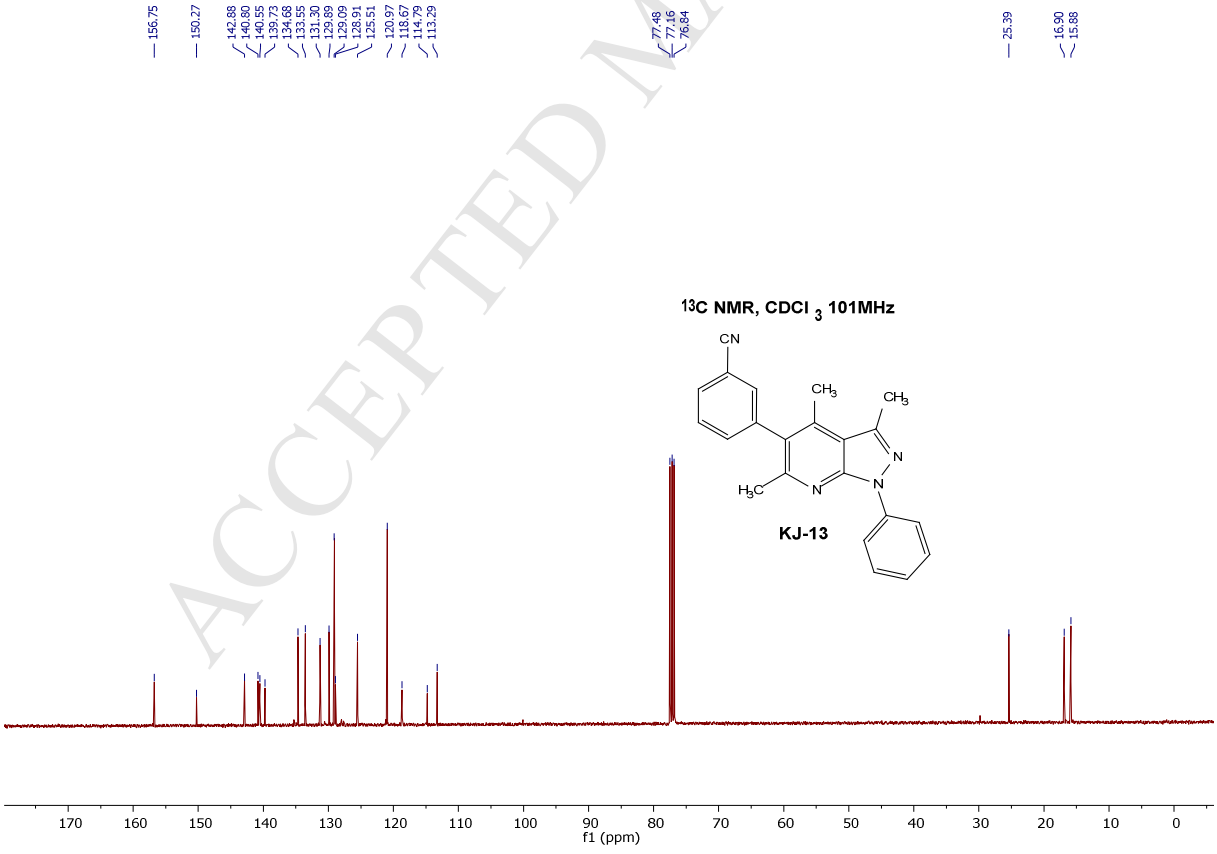

3,4,6-Trimethyl-1-phenyl-5-(thiophen-2-yl)-1H-pyrazolo[3,4-b]pyridine (16).

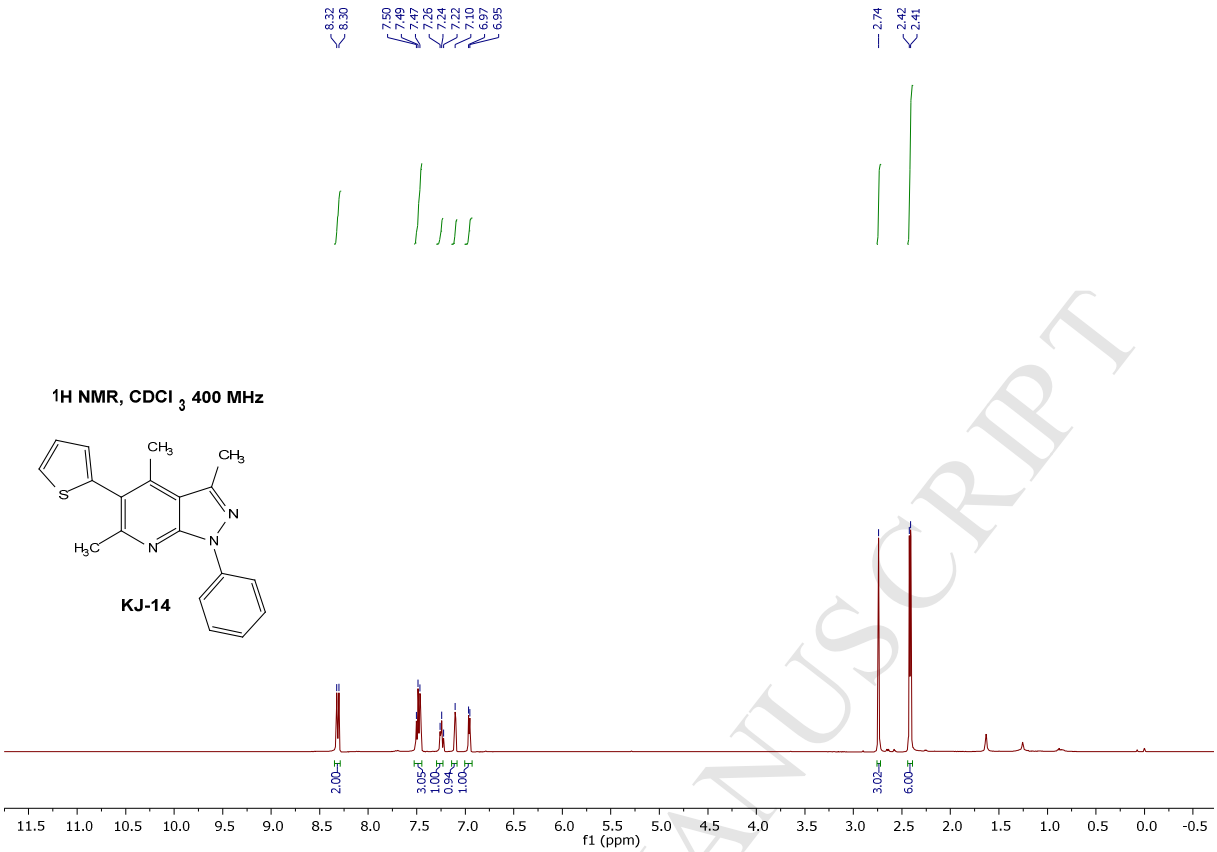

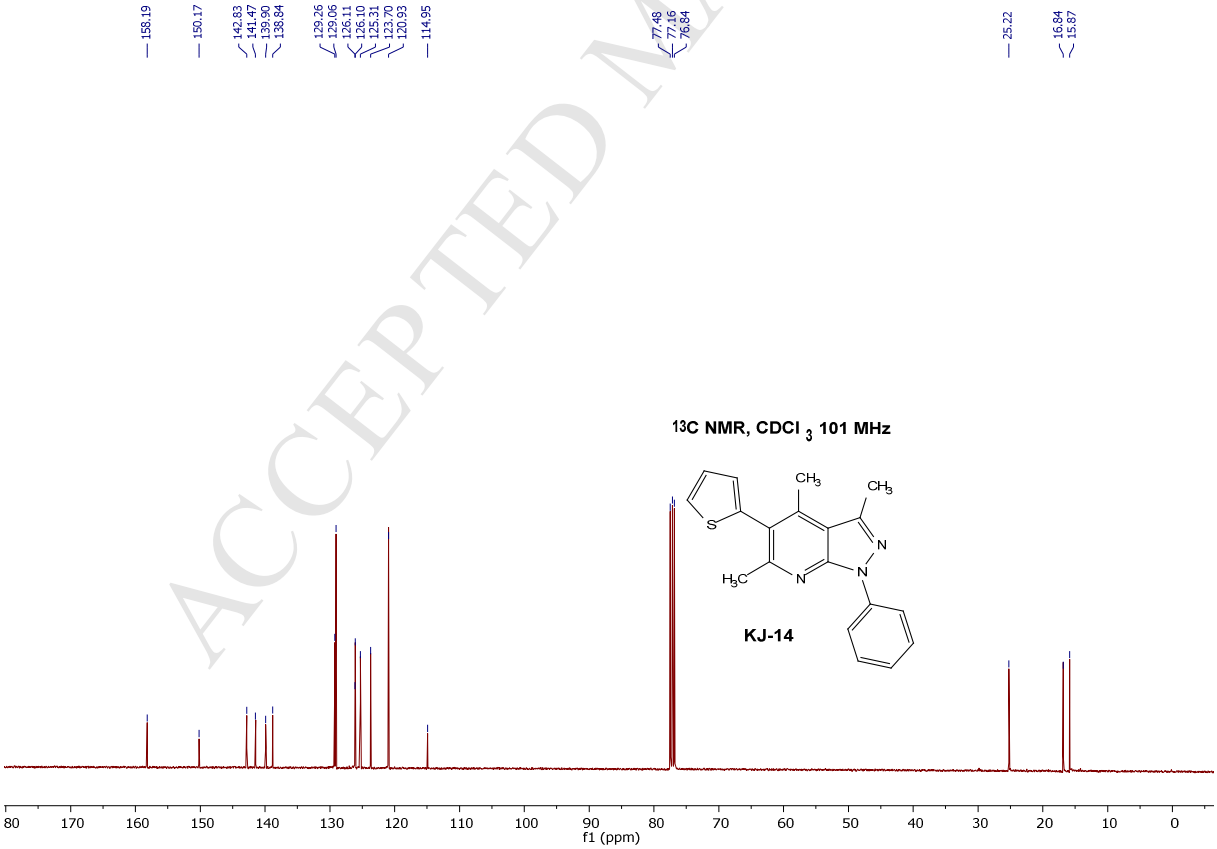

5-(6-Fluoropyridin-3-yl)-3,4,6-trimethyl-1-phenyl-1H-pyrazolo[3,4-b]pyridine (17).

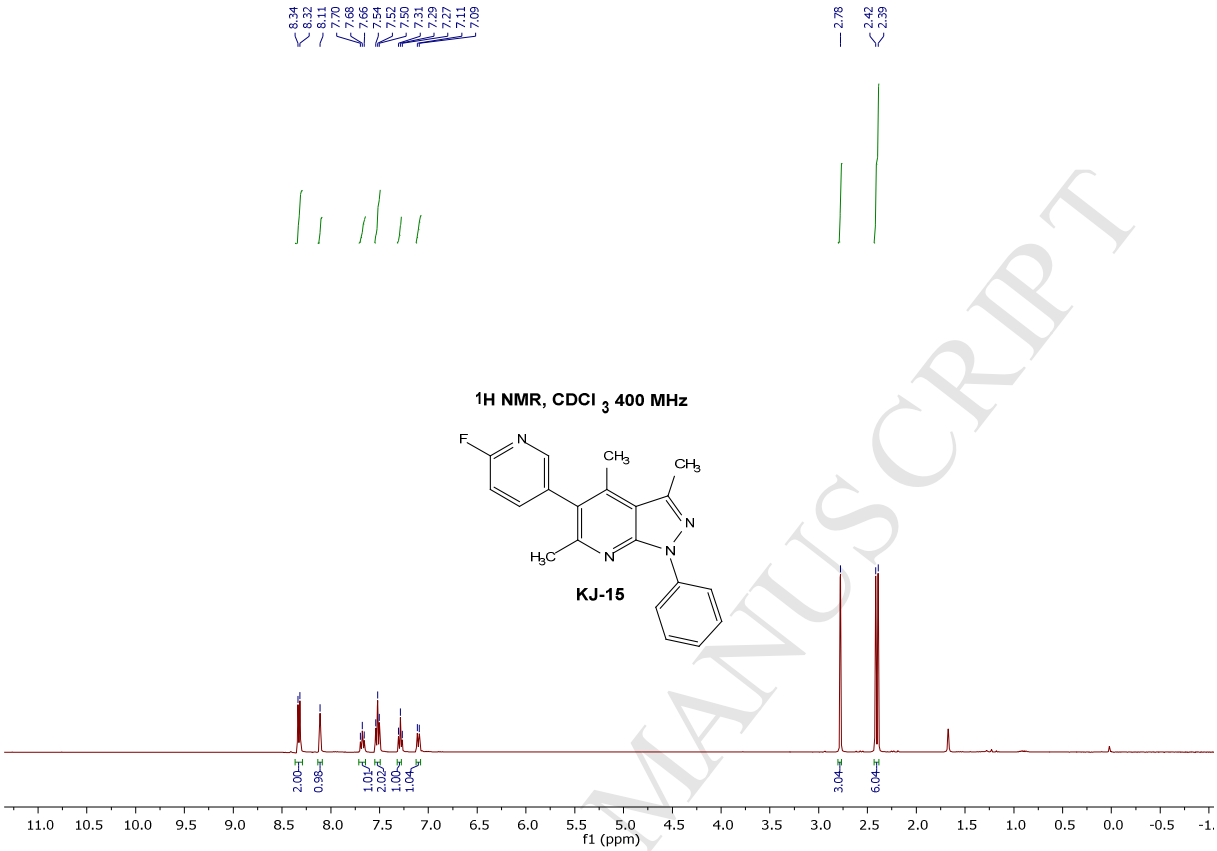

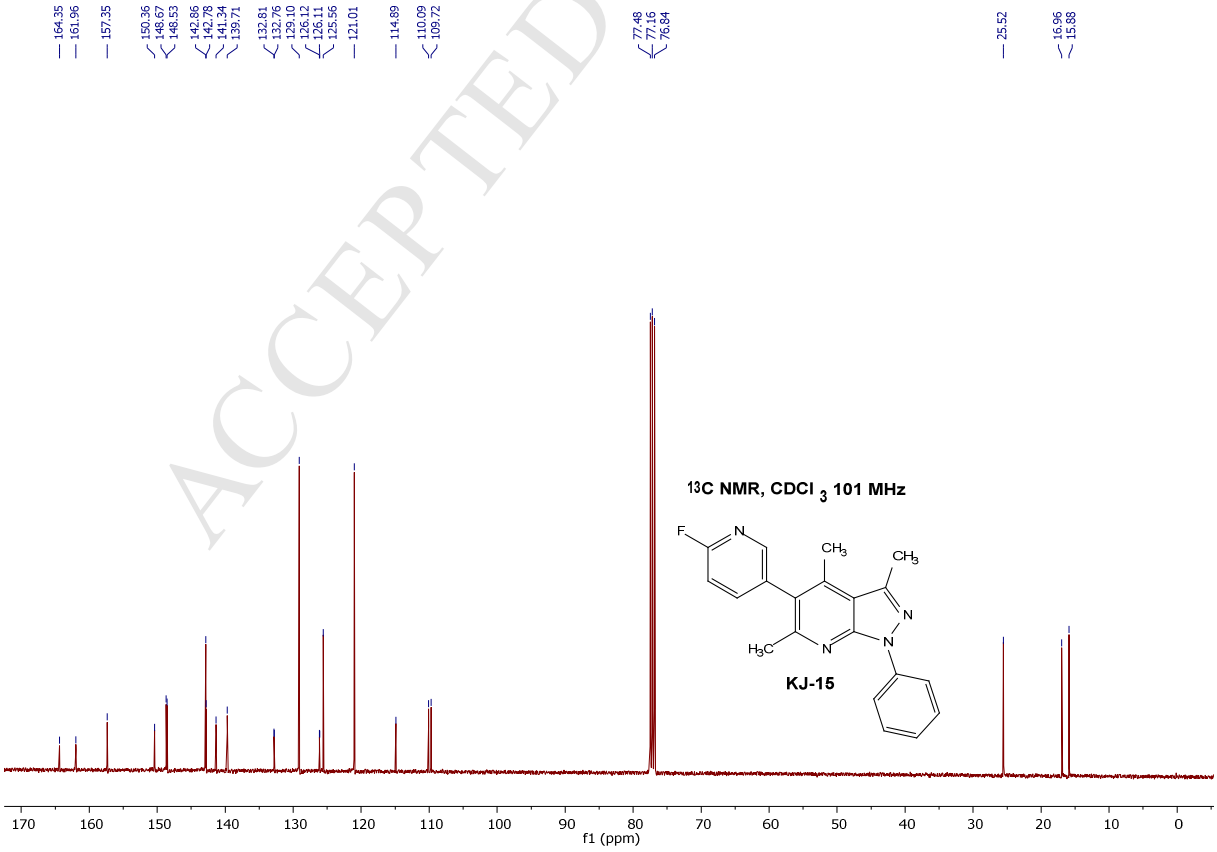

5-(4-Chlorophenyl)-3,4,6-trimethyl-1-phenyl-1H-pyrazolo[3,4-b]pyridine (18).